Running title: OPA1 in LADC

Optic atrophy 1 increases cisplatin resistance via inhibition of caspase-dependent cell death

Hsin-Yuan Fang[1,2], Yu-Ting Wang[3], Kuan-Chih Chow[3,*], Shiow-Her Chiou[4], Hsiu-Ching Yang[3,5], Chih-Yi Chen[5], Tze-Yi Lin[6], I-Ping Chiang[6], Yung-Yen Chiang[7], and Wen-Je Ko[1]

[1]Graduate Institute of Clinical Medicine, National Taiwan University, Taipei, Taiwan, [2]Departments of Surgery, China Medical University Hospital, China Medical University, Taichung, Taiwan, [3]Graduate Institute of Biomedical Sciences and [4]Graduate Institute of Microbiology and Public Health, National Chung Hsing University, Taichung, Taiwan, [5]Comprehensive Cancer Center, China Medical University Hospital, China Medical University, Taichung, Taiwan, [6]Departments of Pathology, China Medical University Hospital, China Medical University, Taichung, Taiwan, [7]Department of Dental Laboratory Technology, Central Taiwan University of Science and Technology, Taichung, Taiwan.

Abstract: word counts, 171; Text: pages 16, word counts: 4226

Table: 1; Figures: 5

*Corresponding author. Graduate Institute of Biomedical Sciences, National Chung Hsing University, 250 Kuo-Kuang Road, Taichung 40227, Taiwan. Tel.: +886-4-22840896 x 118; Fax: +886-4-22859270; E-mail: kcchow@dragon.nchu.edu.tw

Abstract

Optic atrophy 1 (OPA1) protein, a 112-kDa GTPase, is involved in the mitochondrial inner membrane fusion and anticancer drug-mediated cytotoxicity, which implicate an association with disease progression of cancer. In this study we investigated the prognostic value of OPA1 expression in patients with lung adenocarcinomas (LADC). Using immunohistochemical staining, expression of OPA1 was determined in 286 LADC patients. Expression of OPA1 was confirmed by immunoblotting. Relationship between OPA1 expression and clinicopathological parameters was analyzed by a statistical analysis. Difference of survivals between different groups was compared by the log-rank test. The results showed that OPA1 overexpression was detected in 219 (76.6%) of LADC patients. A significant difference was found in cumulative survival between patients with high OPA1 levels and those with low OPA1 levels ($p = 0.0016$). In the in vitro experiments with cell lines, silencing of OPA1 expression decreased cisplatin resistance, which was further shown through increased release of cytochrome c and activation of caspase-dependent pathway. In conclusion, OPA1 is highly expressed in lung adenocarcinomas, and indicates with poor prognosis.

Keywords: mitochondrial inner membrane, fusion, cytochrome c, prognosis, mitochondrial outer membrane, apoptosis-inducing factor

Introduction

Mitochondrion is one of the major organelles responsible for intracellular energy supply and regulation of programmed cell death (Aon *et al*, 2006). Because of the lack of DNA repair mechanism and the necessity to maintain integrity of the genome which encodes only 13 vital proteins for ATP synthesis (Wallace, 1999), mitochondria constantly exchange DNA with one another by fusion and fission (Twig *et al*, 2008). Two proteins, dynamin-related protein 1 (DRP1) and human homolog of yeast mitochondria fission protein 1 (hFis1), are essential for mitochondrial fission (Yoon *et al*, 2003). Three proteins, mitofusin (Mfn)-1, Mfn-2 and optic atrophy 1 (OPA1), are critical for mitochondrial fusion (Cipolat *et al*, 2004). Among them, Mfn-1 and Mfn-2 are imperative for the fusion of the mitochondrial outer membrane (MOM), while OPA1, behaving like its yeast homolog Mgm1, is crucial for the fusion of the mitochondrial inner membrane (Griparic *et al*, 2004).

OPA1 is a dynamin-related guanosine triphosphatase (GTPase). The gene is located on chromosome 3q28-q29, comprising of 31 exons (Davies and Votruba, 2006). The alternative splicing of exons 4, 4b and 5b produces eight transcript variants (http://www.ncbi.nlm.nih.gov/nucleotide/GeneID: 4976). Therefore, depending upon the type of transcript variants the molecular mass of OPA1 has been shown to range from 107- to 118-kDa (924~1015 amino acid residues). Unlike other members of the dynamin family though, OPA1 does not contain the pleckstrin homology region, the GTPase effector domain or the proline-rich stretch at the carboxyl terminus (Chen and Chan, 2005; Davies and Votruba, 2006; Tondera *et al*, 2009). In addition, OPA1 mutations, which are frequently detected in patients with autosomal dominant optic atrophy (ADOA), are correlated with progressive loss of visual acuity, color vision and central vision field, as well as temporal discoloration of optic disc, ascending atrophy and dysmyelination of optic nerve (Chen and Chan, 2005; Davies and Votruba, 2006). In the in vitro experiment, silencing of OPA1

expression by siRNA provokes a series of mitochondrial events, e.g., change of mitochondrial morphology, increase of mitochondrial fragmentation, disruption of mitochondrial cristae as well as release of cytochrome c and induction of apoptosis, suggesting that OPA1 is an anti-apoptotic factor (Olichon *et al*, 2004; Frezza *et al*, 2006; Ishihara *et al*, 2006).

Recently, Todera *et al*. showed that pro-fusion proteins, OPA1 and Mfn-1, were required for cell protection against apoptotic stress induced by actinomycin D or UV irradiation (Olichon *et al*, 2004). Moreover, remodeling of mitochondrial nucleoids, replication complex in mitochondrial matrix of which the structural integrity was maintained by OPA1 and Mfn-1, increased cell resistance to anticancer drug doxorubicin (Garrido *et al*, 2003; Ashley and Poulton, 2009). Interestingly, remodeling of mitochondrial nucleoids is regulated by p53 and ataxia telangiectasia mutated (ATM) protein, indicating that mitochondrial nucleoid and genomic DNA respond to DNA damage in a synchronous fashion. However, OPA1 has not been studied in non-small cell lung cancer, in particular, the lung adenocarcinoma, of which the incidence and mortality have increased dramatically in the last two decades in Taiwan (Annual reports of the Department of Health, the Executive Yuan, Republic of China, 2006). Although cigarette smoking has been shown to be a key factor of disease progression and treatment failure (Chen *et al*, 2006), a portion of patients who do not respond well to the radiation- and chemo-therapy in Taiwan are women and nonsmokers (Toh *et al*, 2006). Treatment failures of LADC, which are associated with DNA repair- and hypoxia-mediated drug- and radiation-resistance as well as with the rapid disease progression (Shannon *et al*, 2003; Chen *et al*, 2006; Toh *et al*, 2006; Maruyama *et al*, 2009), are major causes of the high disease-related mortality.

In this study, we used immunohistochemistry and immunoblotting to determine the expression level of OPA1 in LADC cells and pathological specimens. We also evaluated the statistical correlation between the expression of OPA1 and the clinicopathological parameters

as well as the prognostic significance of OPA1 expression in LADC patients. The effect of OPA1 expression on cisplatin sensitivity was characterized *in vitro*. Our results showed that expression of optic atrophy 1 protein could increase cisplatin resistance, and this effect could be through the inhibition of caspase-dependent cell death in lung adenocarcinoma cells.

Results

Expression of OPA1 in LADC cells determined by RT-PCR

Expression of OPA1 was examined by RT-PCR in one HeLa and nine lung cancer cell lines. OPA1 was detected in all cell lines (Figure 1). Following sequence analysis, which was performed using fluorescence-labeled dideoxy nucleotides (by Mission Biotech, www.missionbio.com.tw, Taipei, Taiwan), and DNA sequencing ladder read by an ABI PRISM 3700 DNA Analyzer (CD Genomics, Shirley, NY, USA), nucleotide sequence homology of cDNA fragments from the nine cell lines matched that of OPA1: BC075805, *Homo sapiens* optic atrophy 1, autosomal dominant (http://blast.ncbi.nlm.nih.gov/Blast.cgi).

Expression of OPA1 in LADC cell lines

Following determination of specificity and sensitivity, monoclonal antibodies were used to detect OPA1 expression in the HeLa and nine lung cancer cell lines. Two protein bands (82- and 110-kDa), corresponding to the anticipated molecular mass of OPA1, were recognized in all the cell lines (Figure 2A). An 82-kDa protein was highly expressed in A549, H520 and H2009 cells. To determine the identity of the two proteins, cell lysate from H520 was precipitated with antibodies to OPA1 and the respective protein bands were subjected to analysis of matrix-assisted laser desorption/ionization-time-of-flight mass spectrometry (MALDI-TOF). The peptide mass fingerprints of both 82-kDa and 110-kDa proteins matched those of OPA1: GenBank| EAW78064.1, optic atrophy 1 (autosomal dominant), isoform CRA a (Homo sapiens). The matched peptides covered 33.8% (325/960 amino acids) of the protein. These data indicated that both 82-kDa and 110-kDa proteins were OPA1 (EAW78064.1) in the LADC cells.

Immunocytochemical staining showed that OPA1 was abundantly present in cytoplasm. The granular appearance of subcellular structures suggested that OPA1 could be present in

mitochondria (Figure 2B). An immunoblotting of sucrose gradient separated organelle fractions confirmed that OPA1 was localized in the mitochondrial fraction (Figure 2C). A MitoTracker® Green (Molecular Probes, Eugene, OR) uptake and confocal fluorescence immunocytochemistry (Figure 2D) further validated that OPA1 was mainly localized in the mitochondria. However, some of OPA1 signals did not co-localize with mitochondria, the grainy appearance suggested that they might be present in other organelles. Using sucrose gradient ultracentrifugation to separate organelle fractions showed that some of OPA1, as determined by immunoblotting, was detected in the mitochondria-associated membrane and light membrane fractions (Figure 2E), in particular when expression of DRP1 or Mfn-2 was inhibited by siRNA, indicating that OPA1 could also be located in the endoplasmic reticulum and mitochondria-associated membrane.

Pathological expression of OPA1 in lung adenocarcinomas

Using immunoblotting, we detected that the major OPA1 expressed in LADC specimens was the 82-kDa OPA1 (Figure 3A). Immunohistochemistry identified OPA1 in 219 (76.6%) of LADC pathological specimens. The signal was predominantly localized in cancer cells (Figure 3B1), but not in the nearby lymphocytes or in the non-tumor lung tissue (NTLT) (Figure 3B2). OPA1 expression was also detected in 54.7% (41/75) of metastatic lymph nodes (data not shown). Statistical analysis showed that overexpression of OPA1 correlated with patient's gender, cigarette smoking habit, tumor stage, lymphovascular invasion, as well as expression of DDH I/II and mitochondria-associated proteins (Table 1), suggesting that OPA1 expression was associated with cell growth and metastatic potential of LADC (21,22). Interestingly, among the 219 patients who had high levels of OPA1, 97 (44.3%) patients had tumor recurrence during follow-up examination. Among the 67 patients who had low levels of OPA1, 8 (11.9%) patients had recurrence. All 105 patients who had recurrence developed

tumors within 24 months after operation. The risk of recurrence for patients with high levels of OPA1 was 3.709-fold higher than that for patients with low levels of OPA1 ($p < 0.001$). Survival of patients with low OPA1 levels was significantly better than that with high OPA1 levels (Figure 3C). The hazard ratio between the 2 groups was 1.69, and the difference in cumulative survival was significant ($p = 0.0016$) by the log-rank test. Multivariate analysis revealed that the difference in OPA1 expression between the 2 groups was highly significant as well ($p = 0.004$).

OPA1 in LADC cells is phosphorylated by PKC, and phosphorylation is essential for maintaining OPA1 stability

Previously, we have shown that phosphorylation of mitochondria-associated proteins, e.g., protein dynamin-related protein 1 (DRP1) and the ATPase family, AAA domain containing 3A (ATAD3A), was critical for maintaining protein stability (Chiang *et al*, 2009; Fang *et al*, 2010). Phosphorylation of DRP1was regulated by hypoxia-related AMP-activating protein kinase (AMPK) and that of ATAD3A was mediated by protein kinase c (PKC). We expected that OPA1 could be phosphorylated as well. We then ran OPA1 sequence through a NetPhos program to predict for phosphorylation sites (http://www.cbs.dtu.dk/services/NetPhos/), and a NetPhosK program to predict for specific kinase (http://www.cbs.dtu.dk/services/NetPhosK/) in eukaryotic proteins, and the results showed that for OPA1 (variant 1) the most probable kinase was PKC at Thr503, Ser708, Thr816, Thr893 and Thr929 (Supplementary Figure S1).

LADC cell lysates were treated with calf intestinal alkaline phosphatase (CIP) before immunoblotting, the amount of the 110-kDa protein was reduced, but that of the 82-kDa protein was increased (Figure 4A). These results suggest that the110-kDa OPA1 could be a phosphorylated form. LADC cells were therefore treated with a panel of kinase inhibitors. As shown in Figure 4B, addition of calphostin C, a PKC inhibitor, reduced the intensity of

82-kDa and 110-kDa protein bands, indicating that PKC was the kinase for OPA1 phosphorylation, and that phosphorylation was essential for maintaining OPA1 stability. For identifying the PKC isozyme that was responsible for OPA1 phosphorylation, H2009 cells, which expressed intermediate levels of OPA1, were transfected with plasmids carrying various genes of PKC isozyme. Interestingly, levels of the 110-kDa protein increased in cells expressed ectopical PKC isozymes (Figure 4C). These results confirmed that PKC was accountable for OPA1 phosphorylation. Addition of 10 μM nicotine at 37°C for 4 h increased levels of 110-kDa OPA1 (Figure 4D) and cisplatin resistance (Figure 4E).

Biosynthesis of OPA1 increases during S phase of cell cycle progression and silencing of OPA1 expression increases drug sensitivity

PKC activity is frequently associated with growth factor receptor-related cellular events and cell cycle progression (Hirai *et al*, 1989; Black, 2000). Therefore, findings of PKC involvement in OPA1 phosphorylation suggested that OPA1 expression could be regulated by a cell cycle progression- or a growth factor receptor-related pathway. We therefore studied OPA1 expression pattern during cell cycle progression by the serum starvation-reactivation and the double-thymidine block methods. Results of double-thymidine block and release showed that levels of OPA1 protein, like other mitochondria-related proteins, e.g., DRP1 and ATAD3A (21, 22), increased during the S phase (four hours after release from DTB) and decreased in the G1 phase (16 hours after release from DTB) (Figure 5A), indicating that biosynthesis of OPA1 was during the S phase of cell cycle progression. Serum starvation markedly reduced 110-kDa OPA1 (Figure 5B). Replenish of serum increased both the 82- and 110-kDa proteins, suggesting that in addition to cell cycle progression OPA1 expression was regulated by growth factor receptor-related proliferation stimulation as well, by which OPA1 appeared rapidly following serum re-activation.

Previous studies have suggested that OPA1 plays an anti-apoptotic role in response to stress challenge (Garrido *et al*, 2006; Ashley and Poulton, 2009). As anticipated, knockdown of OPA1 ($OPA1^{kd}$) expression by siRNA (Figure 5C) increased cisplatin sensitivity (Figure 5D). The effect of OPA1 silencing on cisplatin sensitivity persisted through cell cycle (Figure 5E). Very little cytotoxicity was observed in H23 cells until 12 hrs post serum stimulation. Maximal cell killing occurred between 15-21 hrs after serum re-activation, but around 24 hrs there was again a reduction in cisplatin cytotoxicity. Reduction of OPA1 expression increased 5-30% of cisplatin sensitivity, suggesting that besides nuclear toxicity, cisplatin might have toxicity to mitochondria as well. Results of confocal fluorescence immunocytochemistry (Figure 5F) and immunoblotting of sucrose gradient-separated organelle fractions (Figure 5G) showed that OPA1 silencing increased cytoplasmic cytochrome c, but not cytoplasmic nor nuclear apoptosis-inducing factor (AIF) following staurosporine (STS) treatment, suggesting that OPA1 deficiency might increase caspase-dependent cell death. We added sub-lethal doses of STS to examine this postulation. Interestingly, although treatment with sub-lethal doses of STS provoked very diminutive effect on caspase 3 activation (Figure 5H1) or degradation of poly (ADP-ribose) polymerase (PARP) (Figure 5H2) in wild-type A540 cells, it did induce greater effect on enzyme activation and substrate disintegration of caspase-dependent cell death.

Discussion

Our results show that OPA1expression is frequently elevated in LADC. Increased OPA1 expression in LADC patients significantly correlates with patient's gender, cigarette smoking habit, tumor stage and higher incidence of tumor recurrence as well as reduced drug sensitivity, all of which indicate poor prognosis.

As shown in the immunoblotting experiment, besides an 82-kDA protein, OPA1 signals of size between 82- and 110-kDa were detected in both the pathological specimens and LADC cell lines. After CIP treatment, the intensity of the protein bands above 82-kDa reduced and that of the 82-kDa protein increased, indicating that the protein bands above 82-kDa OPA1 was phosphorylated. However, the 82-kDa protein was also sensitive to CIP, suggesting that the 82-kDa OPA1 was phosphorylated as well. Treatment with calphostin C, a pan-PKC inhibitor, reduced phosphorylation and protein level of 82- and 110-kDa OPA1, further implying that PKC could be the kinase that catalyzes OPA1 phosphorylation (Kobayashi *et al*, 1989), and that post-translational modification is essential for maintaining OPA1 stability. Ectopic PKC expression showed that all the PKC isozymes were capable for OPA1 phosphorylation. These data corresponded well with the current results of clinicopathological analyses that OPA1 expression correlated with patient's habit of cigarette smoking, which could directly or indirectly influence PKC activity (Gopalakrishna *et al*, 1994; Lee *et al*, 2001).

Moreover, PKC activity is frequently associated with growth factor receptor-related cellular events and cell cycle (Hirai *et al*, 1989; Black, 2000; Fima *et al*, 2001). By showing that OPA1 expression is up-regulated during S phase of cell cycle progression and that OPA1 is phosphorylated by PKC, our work suggests that phosphorylation may be a general mechanism for maintaining protein stability. These data also support our recent findings that mitochondria-related proteins, e.g., DRP1 and ATAD3A, of which the expression is elevated

during S phase, are phosphorylated by PKC, and associated with increased drug resistance (Chiang *et al*, 2009; Fang *et al*, 2010). It is therefore worth noting that knockdown of OPA1 expression by siRNAs ($OPA1^{kd}$) decreased cisplatin resistance. These results clearly indicate that the OPA1 plays an important role in the drug sensitivity of LADC, which then reflects in patient's survival. Patients with low OPA1 level are more sensitive to cisplatin-based chemotherapy and have a better prognosis. In contrast, those with high OPA1 level are more resistant to chemotherapy and, thus, have a poorer prognosis. The exact mechanism by which OPA1 contributes to cisplatin resistance, however, is not yet clear.

By showing that antioxidants delayed the onset of mitochondrial dysfunction in $OPA1^{+/-}$ drosophila, Tang et al. suggested that OPA1 mutations increased the production of oxygen reactive species (ROS) (Tang *et al*, 2009). Using electron microscopy, Olichon et al. showed that OPA1 deficiency led to perturbation of both mitochondrial inner and outer membranes (Olichon *et al*, 2003), implying that OPA1 could be essential for maintaining the mitochondrial membrane integrity and for preventing ROS leakage (Olichon *et al*, 2003; Griparic *et al*, 2004). High intracellular level of ROS might initiate the aberrant autophagic cell death (White *et al*, 2009). Interestingly, ROS induced AKR1C2 expression *via* activation of antioxidant response element (Burczynski *et al*, 200335, Lou *et al*, 2006), and AKR1C1/2 overexpression was frequently detected in LADC (Hsu *et al*, 2001). It is possible that in the absence of polycyclic aromatic hydrocarbons (PAH), AKR1C1/2 may catabolize the excessive endogenous or cisplatin-induced ROS (Deng *et al*, 2002). It is worth noting that aldoketo reductase contains PGF synthase activity and $PGF_{2\alpha}$ level is proportional to AKR1C expression (Nakashima *et al*, 2003; Wang *et al*, 2007). AKR1C is a down-stream enzyme of cytochrome p450 1A1 and epoxide hydrolase, which convert hydroxylated PAH into catechols (Vogel *et al*, 1980). When cells were under hypoxic condition, the reduced intracellular oxygen would exhaust the supply of dihydrodiol derivatives of PAH, and redirect

AKR1C to catalyze the intrinsic substrates toward prostaglandin F (PGF) synthesis. In addition to the elevated synthesis of $PGF_{2\alpha}$, hypoxia increased expression of hepatocyte growth factor (HGF) and interleukin (IL)-8 as well (Chiang, 2009). HGF, IL-8 and $PGF_{2\alpha}$ consequently induced cancer cell's growth and metastasis during disease progression (Chen *et al*, 2006; Chiang, 2009). Our results not only supported the recent findings by Seo et al. that AKR1C1/2 was highly expressed in the cancer stem cell population of LADC cell line A549 (Seo *et al*, 2007), but also provided a reasonable explanation for the increased drug resistance and elevated proliferation in cancer stem cells (Hsu *et al*, 2001; Shannon *et al*, 2006; Chen *et al*, 2006), suggesting that overexpression of AKR1C1/2 and OPA1 could be key features of cancer stem cells.

In fact, mitochondria are one of the major intracellular targets for clinically important anticancer drugs, such as cisplatin (Yang *et al*, 1997) and etoposide (Park and Kim, 2005). Current evidence suggests that in addition to the nuclear targets, these drugs may directly influence mitochondrial membrane functions, which are imperative for preventing the release of cytotoxic cytochrome c to initiate caspase-dependent cell death. The present study sheds further light on the status of mitochondrial OPA1protein in the cell cycle and how this affects cisplatin sensitivity. The increased cisplatin sensitivity in $OPA1^{kd}$ cells when compared to those which are logarithmically growing is consistent with the observations of others that OPA1, like ATAD3A and DRP1, could be an anti-apoptotic factor (Olichon *et al*, 2006; Chiang *et al*, 2009; Fang *et al*, 2010). Moreover, our results suggest that mitochondria and nucleus may have different effects on drug sensitivity of the cells. Elegant studies by Olichon *et al* and Griparic *et al* showed that OPA1 deficiency increased deformation of mitochondria , inflation of mitochondrial cristae and abrasion of MOM (Olichon *et al*, 2003; Griparic *et al*, 2004), indicating that in addition to mitochondrial inner membrane fusion OPA1 might have a role for maintaining the integrity of MOM, i.e., by reducing ROS-associated membrane

damage or facilitating the phospholipid supply for MOM (Fang *et al*, 2010). The MOM abrasion increased the release of cytochrome c (caspase-dependent cell death), but not AIF (caspase-independent cell death), when cells were challenged with genotoxic stress, supporting the report by Frezza *et al* that OPA1 guarded the corralled cytochrome c in the enclosed cristae (Frezza *et al*, 2006). The mechanisms of differential release of cytochrome c and AIF, however, remain to be resolved.

In conclusion, immunoblotting and immunohistochemical staining reveal abundant expression of OPA1 in the LADC cells. Pathological results indicate that OPA1 expression correlates with patient's gender, cigarette smoking habit, tumor stage and expression of AKR1C1/2, the features which are closely associated with the increased drug resistance and metastatic potential as well as the poor prognosis. In the in vitro experiments using LADC cells, our results show that OPA1 expression is tightly regulated during cell cycle, and OPA1 is phosphorylated by PKC. Silencing of OPA1 expression increases the level of cisplatin sensitivity, possibly via caspase-dependent cell death pathway, in LADC cell lines.

Materials and Methods

Tissue specimens and lung adenocarcinoma cell (LADC) lines

From January 2001 to December 2004, tissue specimens were collected from 286 patients with newly diagnosed LADC. Samples from all patients, for whom at least one follow-up examination or death was documented, were pathologically confirmed LADC. The stage of the disease was classified according to the new international staging system for lung cancer (Detterbeck *et al*, 2009). The protocols of these studies had been approved by the Medical Ethics Committee at China Medical University Hospital (DMR99-IRB-062).

Nine NSCLC cell lines (H23, H125, H226, H838, H1437, H2009, H2087, A549 and H520) were used for the in vitro evaluation of gene expression. H23, H838, H1437, H2009, H2087 and A549 are LADC cells, and H125, H226 and H520 are epithelial type cells. Cells were grown at 37°C in a monolayer in RPMI 1640 supplemented with 10% fetal calf serum (FCS), 100 I.U./ml penicillin and 100 μg/ml streptomycin.

Reverse transcription-polymerase chain reaction (RT-PCR)

Following total RNA extraction and synthesis of the first-strand cDNA, an aliquot of cDNA was subjected to 35 cycles of PCR to determine the integrity of β-actin mRNA (Chen *et al*, 2006). The cDNA used in the following RT-PCR was adjusted according to the quality and quantity of β-actin mRNA. The primer sequences were selected by the web software Primer3 (http://frodo.wi.mit.edu/cgi-bin/primer3). For all the OPA1 variants, the primers are: OPA1s: 5'-GGAACAGCTCTGAAAGCATT-3' [sense primer, nucleotides (nts) 1737-1756, NM_130837.1] and OPA1a: 5'-AACTTTCTTGAGGTCTTCCG-3' (antisense primer, nts 3046-3027). The anticipated cDNA fragments are 1310 bp. For differentiating OPA1 variants, the primers are: OPA1vs: 5'-GGATTGTGCCTGACATTGTG-3' (sense primer, nts 456-475, NM_130837.1) and OPA1va: 5'-TGCCTTTGTCATCTTTCTGC-3' (antisense primer, nts

983-964). The anticipated cDNA fragments are 528 bp (variant 8), 474 bp (variant 7), 420 bp (variant 6), 417 bp (variant 5), 366 bp (variant 4), 363 bp (variant 1), 309 bp (variant 3) and 255 bp (variant 2).

Immunoprecipitation, gel electrophoresis and protein analysis by MALDI-TOF

Total cell lysate was prepared by mixing 5×10^7 cells/100 μl phosphate-buffered saline with equal volume of 2 × NP-40 lysis buffer [40 mM Tris-HCl, pH 7.6, 2 mM EDTA, 300 mM NaCl, 2% NP-40, and 2 mM phenylmethylsulfonylfluoride (PMSF)]. Protein G sepharose™ (Amersham Biosciences AB, Uppsala, Sweden) was pre-washed before mixing with 500 μg of total cell lysate. The reaction mixture was incubated at 4°C for 60 minutes, and then centrifuged at 800 × g for 1 minute. The supernatant was reacted with 5 μg of purified monoclonal antibodies and 20 μl of fresh protein G sepharose at 4°C for 18 hours. The reaction mixture was centrifuged at 800 × g for 1 minute. Following removal of the supernatant, the precipitate was washed with 1 × PBS, and dissolved in loading buffer (50 mM Tris, pH 6.8, 150 mM NaCl, 1 mM disodium EDTA, 1 mM PMSF, 10% glycerol, 5% β-mercaptoethanol, 0.01% bromophenol blue and 1% SDS). Eletrophoresis was carried out in two 10% polyacrylamide gels with 4.5% stacking. One gel was processed for immunoblotting (Chen *et al,* 2006), and the other gel was stained with Coomassie blue. Protein bands on the Coomassie-stained gel, which corresponded to the immunoblotting-positive bands, were extracted from the gel for identification by MALDI-TOF on a Voyager-DE™ pro biospectrometry workstation (Applied Biosystems, Milpitas, CA, USA). Fragments of peptide fingerprints were matched with those on the SwissProt database by MS-fit (ProteinProspector 4.0.5., The Regents of the University of California). After electrophoresis, proteins on the first gel were transferred to a nitrocellulose membrane for immunoblotting. The membrane was probed with specific antibodies. The signal was amplified by

biotin-labeled goat anti-mouse IgG, and peroxidase-conjugated streptavidin. The protein was visualized by exposing the membrane to an X-Omat film (Eastman Kodak, Rochester, NY) with enhanced chemiluminescent reagent (NEN, Boston, MA).

Immunoblotting analysis and immunostaining

Immunoblotting and immunohistochemistry were performed as described previously (Chen *et al*, 2006). Antibodies for β-actin were obtained from Chemicon International (Temecula, CA). Antibodies to OPA1 were raised in the laboratory. For immunocytochemical staining, the cells were grown overnight on slide, and then fixed with cold methanol/acetone at 4°C for 10 minutes before staining. For and immunohistochemical staing, the pathological slides were processed by a routine procedure. Following inactivation of endogenous peroxidase, the immunological staining was performed by an immunoperoxidase method (Chen *et al*, 2006). Antibodies for aldoketo reductase (AKR) 1C1/2 [also called dihydrodiol dehydrogenase (DDH) I/II], DRP1, ATAD3A, Mfn-1 and Mfn-2 were raised and characterized in our laboratory (Lin, 2005; Chiang *et al*, 2009; Fang *et al*, 2010). Antibodies to OPA1 were not added for the negative control group.

Slide evaluation of OPA1 expression by immunohistochemical staining

In each pathological section, non-tumor lung tissue served as internal negative control. Slides were evaluated by two independent pathologists blinded to the clinicopathological knowledge. The ImmunoReactive Scoring system was adapted for this study (Remmele and Schicketanz, 1993). Briefly, a specimen was considered having strong signals when more than 50% of cancer cells were positively stained; intermediate, if 25-50% of the cells stained positive; weak, if less than 25% or more than 10% of the cells were positively stained; and negative, if less than 10% of the cancer cells were stained. Cases with strong and intermediate OPA1

signals were classified as $OPA1^+$, and those with weak or negative OPA1 signals were classified as $OPA1^-$ (Chen *et al*, 2006; Chiang *et al*, 2009).

Colony assay

Cells were treated at different time point during serum stimulation with various concentration of cisplatin at 37°C for 4 h, wash twice with warm medium for 10 min, and then trypsinized. Viable cells, as determined by trypan blue dye exclusion, were seeded quantitatively into 6-well plates with 5 ml of medium and incubated at 37°C and in 5% CO_2 over 7-10 days. Colonies were stained with 2% crystal violet in methanol (with 3% glacial acetic acid). Percent survival was determined by comparison to PBS-treated controls. For gene silencing experiments, cells were harvested 48 hours following siRNA treatment.

Statistical analysis

Correlation of OPA1 level with clinicopathological factors was analyzed by either the Chi-Square test or the Fisher's exact test. Survival curves were plotted using the Kaplan-Meier estimator (Kaplan and Meier, 1958). Statistical difference in survival between different groups was compared by the log rank (Mantel, 1966) test. Statistical analysis was performed using GraphPad Prism5 statistics software (San Diego, CA). Statistical significance was set at $p < 0.05$.

Acknowledgements

This study was supported, in part, by the Comprehensive Academic Promotion Projects, Department of Education (NCHU 995002 to K.C. Chow), and, in part, by the Taiwan Department of Health, China Medical University Hospital, Cancer Research of Excellence (DOH99-TD-C-111-005). RNAi for silencing OPA1 gene expression was obtained from the National RNAi Core Facility in the Institute of Molecular Biology/Genomic Research Center, Academia Sinica, Taipei, Taiwan, supported by the National Research Program for Genomic Medicine Grants of NSC (NSC 97-3112-B-001-016).

Conflict of interest

The authors declare that they have no conflict of interest.

References

Aon MA, Cortassa S, Akar FG, O'Rourke B (2006) Mitochondrial criticality: a new concept at the turning point of life or death. *Biochim Biophys Acta* **1762**: 232-240

Ashley N, Poulton J (2009) Anticancer DNA intercalators cause p53-dependent mitochondrial DNA nucleoid re-modelling. *Oncogene* **28**: 3880-3891

Black JD (2000) Protein kinase C-mediated regulation of the cell cycle. *Front Biosci* **5**: D406-423

Burczynski ME, Lin HK, Penning TM (1999) Isoform-specific induction of a human aldo-keto reductase by polycyclic aromatic hydrocarbons (PAHs), electrophiles, and oxidative stress: implications for the alternative pathway of PAH activation catalyzed by human dihydrodiol dehydrogenase. *Cancer Res* **59**: 607-614

Chen H, Chan DC (2005) Emerging functions of mammalian mitochondrial fusion and fission. *Hum Mol Genet* 14: R283-289

Chen JT, Lin TS, Chow KC, Huang HH, Chiou SH, Chiang SF, Chen HC, Chuang TL, Lin TY, Chen CY (2006) Cigarette smoking induces overexpression of HGF in type II pneumocytes and lung cancer cells. *Am J Respir Cell Mol Biol* **34**: 264-273

Chiang YY (2009) Hepatocyte growth factor induces hypoxia-related interleukin-8 expression in lung adenocarcinoma cells. *Mol Carcinog* **48**: 662-670

Chiang YY, Chen SL, Hsiao YT, Huang CH, Lin TY, Chiang IP, Hsu WH, Chow KC (2009) Nuclear expression of dynamin-related protein 1 in lung adenocarcinomas. *Mod Pathol* **22**: 1139-1150

Cipolat S, Martins de Brito O, Dal Zilio B, Scorrano L (2004) OPA1 requires mitofusin 1 to promote mitochondrial fusion. *Proc Natl Acad Sci USA* **101**: 15927-15932

Davies V, Votruba M (2006) Focus on molecules: the OPA1 protein. *Exp Eye Res* **83**: 1003-1004

Deng HB, Parekh HK, Chow KC, Simpkins H (2002) Increased expression of dihydrodiol dehydrogenase induces resistance to cisplatin in human ovarian carcinoma cells. *J Biol Chem* **277**: 15035-15043

Detterbeck FC, Boffa DJ, Tanoue LT (2009) The new lung cancer staging system. *Chest* **136**: 260-271

Fang HY, Chang CL, Hsu SH, Huang CY, Chiang SF, Chiou SH, Huang CH, Hsiao YT, Lin TY, Chiang IP, Hsu WH, Sugano S, Chen CY, Lin CY, Ko WJ, Chow KC (2010) ATPase family AAA domain-containing 3A is a novel anti-apoptotic factor in lung adenocarcinoma cells. *J Cell Sci* **123**: 1171-1180

Fima E, Shtutman M, Libros P, Missel A, Shahaf G, Kahana G, Livneh E (2001) PKCeta enhances cell cycle progression, the expression of G1 cyclins and p21 in MCF-7 cells. *Oncogene* **20**: 6794-6804

Frezza C, Cipolat S, Martins de Brito O, Micaroni M, Beznoussenko GV, Rudka T, Bartoli D, Polishuck RS, Danial NN, De Strooper B, Scorrano L (2006) OPA1 controls apoptotic cristae remodeling independently from mitochondrial fusion. *Cell* **126**: 177-189

Garrido N, Griparic L, Jokitalo E, Wartiovaara J, van der Bliek AM, Spelbrink JN (2003) Composition and dynamics of human mitochondrial nucleoids. *Mol Biol Cell* **14**: 1583-1596

Gopalakrishna R, Chen ZH, Gundimeda U (1994) Tobacco smoke tumor promoters, catechol and hydroquinone, induce oxidative regulation of protein kinase C and influence invasion and metastasis of lung carcinoma cells. *Proc Natl Acad Sci USA* **91**: 12233-12237

Griparic L, van der Wel NN, Orozco IJ, Peters PJ, van der Bliek AM (2004) Loss of the intermembrane space protein Mgm1/OPA1 induces swelling and localized constrictions along the lengths of mitochondria. *J Biol Chem* **279**: 18792-18798

Hirai M, Gamou, S, Kobayashi M, Shimizu N (1989) Lung cancer cells often express high levels of protein kinase C activity. *Jpn J Cancer Res* **80**: 204-208

Hsu NY, Ho HC, Chow KC, Lin TY, Shih CS, Wang LS, Tsai CM (2001) Overexpression of dihydrodiol dehydrogenase as a prognostic marker of non-small cell lung cancer. *Cancer Res* **61**: 2727-2731

Ishihara N, Fujita Y, Oka T, Mihara K (2006) Regulation of mitochondrial morphology through proteolytic cleavage of OPA1. *EMBO J* **25**: 2966-2977

Kaplan EL, Meier P (1958) Nonparametric estimation from incomplete observations. *J Am Stat Assoc* **53**: 457-481

Kobayashi E, Nakano H, Morimoto M, Tamaoki T (1989) Calphostin C (UCN-1028C), a novel microbial compound, is a highly potent and specific inhibitor of protein kinase C. *Biochem Biophys Res Commun* **159**: 548-553

Lee SD, Lee DS, Chun YG, Shim TS, Lim CM, Koh Y, Kim WS, Kim DS, Kim WD (2001) Cigarette smoke extract induces endothelin-1 via protein kinase C in pulmonary artery endothelial cells. *Am J Physiol Lung Cell Mol Physiol* **281**: L403-L411

Lin MY (2005) Expression of mitofusins in non-small cell lung cancer. Master thesis, Graduate Institute of Biomedical Sciences, National Chung Hsing University, Taichung, Taiwan.

Lou H, Du S, Ji Q, Stolz A (2006) Induction of AKR1C2 by phase II inducers: identification of a distal consensus antioxidant response element regulated by NRF2. *Mol Pharmacol* 69: 1662-1672

Mantel N (1966) Evaluation of survival data and two new rank order statistics arising in its consideration. *Cancer Chemother Rep* **50**: 163-170

Maruyama R, Wataya H, Seto T, Ichinose Y (2009) Treatment after the failure of gefitinib in patients with advanced or recurrent non-small cell lung cancer. *Anticancer Res* 29: 4217-4221

Nakashima K, Ueno N, Kamei D, Tanioka T, Nakatani Y, Murakami M, Kudo I (2003) Coupling between cyclooxygenases and prostaglandin F(2alpha) synthase. Detection of an inducible, glutathione-activated, membrane-bound prostaglandin F(2alpha)-synthetic activity. *Biochim Biophys Acta* **1633**: 96-105

Olichon A, Baricault L, Gas N, Guillou E, Valette A, Belenguer P, Lenaers G (2003) Loss of OPA1 perturbates the mitochondrial inner membrane structure and integrity, leading to cytochrome c release and apoptosis. *J Biol Chem* **278**: 7743-7746

Park JH, Kim TH (2005) Release of cytochrome c from isolated mitochondria by etoposide. *J Biochem Mol Biol* **38**: 619-623

Remmele W, Schicketanz KH (1993) Immunohistochemical determination of estrogen and progesterone receptor content in human breast cancer. Computer-assisted image analysis (QIC score) vs. subjective grading (IRS). *Pathol Res Pract* **189**: 862-866.

Seo DC, Sung JM, Cho HJ, Yi H, Seo KH, Choi IS, Kim DK, Kim JS, El-Aty AM A, Shin HC (2007) Gene expression profiling of cancer stem cell in human lung adenocarcinoma A549 cells. *Mol Cancer* **6**: 75-82

Shannon AM, Bouchier-Hayes DJ, Condron CM, Toomey D (2003) Tumor hypoxia, chemotherapeutic resistance and hypoxia-related therapies. *Cancer Treat Rev* **29**: 297-307

Tang S, Le PK, Tse S, Wallace DC, Huang T (2009) Heterozygous mutation of Opa1 in Drosophila shortens lifespan mediated through increased reactive oxygen species production. *PLoS One* **4**: e4492.

Toh CK, Gao F, Lim WT, Leong SS, Fong KW, Yap SP, Hsu AA, Eng P, Koong HN, Thirugnanam A, Tan EH (2006) Never-smokers with lung cancer: epidemiologic evidence of a distinct disease entity. *J Clin Oncol* **24**: 2245-2251

Tondera D, Grandemange S, Jourdain A, Karbowski M, Mattenberger Y, Herzig S, Da Cruz S, Clerc P, Raschke I, Merkwirth C, Ehses S, Krause F, Chan DC, Alexander C, Bauer C, Youle R, Langer T, Martinou JC (2009) SLP-2 is required for stress-induced mitochondrial hyperfusion. *EMBO J* **28**: 1589-1600

Twig G, Hyde B, Shirihai OS (2008) Mitochondrial fusion, fission and autophagy as a quality control axis: the bioenergetic view. *Biochim Biophys Acta* **1777**: 1092-1097

Vogel K, Bentley P, Platt KL, Oesch F (1980) Rat liver cytoplasmic dihydrodiol dehydrogenase. *J Biol Chem* **255**: 9621-9625

Wallace DC (1999). Mitochondrial diseases in man and mouse. *Science* **283**: 1482-1488.

Wang HW, Lin CP, Chiu JH, Chow KC, Kuo KT, Lin CS, Wang LS (2007) Reversal of inflammation-associated dihydrodiol dehydrogenases (AKR1C1 and AKR1C2) overexpression and drug resistance in nonsmall cell lung cancer cells by wogonin and chrysin. *Int J Cancer* **120**: 2019-2027

White KE, Davies VJ, Hogan VE, Piechota MJ, Nichols PP, Turnbull DM, Votruba M (2009) OPA1 deficiency associated with increased autophagy in retinal ganglion cells in a murine model of dominant optic atrophy. *Invest Ophthalmol Vis Sci* **50**: 2567-2571

Yang J, Liu X, Bhalla K, Kim CN, Ibrado AM, Cai J, Peng TI, Jones DP, Wang X (1997) Prevention of apoptosis by Bcl-2: release of cytochrome c from mitochondria blocked. *Science* 275: 1129-1132

Yoon Y, Krueger EW, Oswald BJ, McNiven MA (2003) The mitochondrial protein hFis1 regulates mitochondrial fission in mammalian cells through an interaction with the dynamin-like protein DLP1. *Mol Cell Biol* **23**: 5409-5420

Figure legends

Figure 1 Expression of OPA1 detected by RT-PCR in cancer cells. Expression of OPA1 mRNA was detected by RT-PCR in one HeLa and eight LADC cell lines. Expression of β-actin was used as a monitoring standard for the relative expression ratio of OPA1 mRNA.

Figure 2 Characterization of monoclonal antibodies to OPA1. **(A)** Immunoblotting revealed that monoclonal antibodies raised against recombinant OPA1 recognized 2 protein bands of approximately 95-kDa. Expression of the 82-kDa OPA1 was detected in all nine human lung cancer cell lines, high in H520, intermediate in H23, H125, H226, H1437, H2009, H2087 and A549 (relative to H838), and low in H838 cells. Expression of the 110-kDa protein was detected in eight human lung cancer cell lines, but not in H2009 cells. Cell lysate from H23 were precipitated by OPA1-specific monoclonal antibodies and protein G sepharose™. Both the 82- and 110-kDa proteins were characterized by MALDI-TOF. The peptide mass fingerprints of 82-kDa and 110-kDa proteins matched that of OPA1: MS-Fit search (http://prospector.ucsf.edu/): EAW78064.1, optic atrophy 1 (autosomal dominant), isoform CRA a (Homo sapiens). (**B**) Immunocytochemical staining showed that OPA1 was abundantly present as distinct granules in the cytoplasm of A549 cells, which suggests that OPA1 is located in mitochondria. (**C**) Immunoblotting of H23 subcellular fractions, which were separated by sucrose gradient ultracentrifugation. Cytosol, cytosolic fraction; COX IV, cytochrome c Oxidase IV of mitochondria; (**D**) Confocal fluorescence immunocytochemical staining of A549 cells. OPA1 was detected by specific monoclonal antibodies labeled with FITC. Mitochondria were labeled with MitoTracker® Red CMXRos dye. Nuclei were stained with fluorescent dye 4', 6-diamidino-2-phenylindole (DAPI). A merged image of the first, second and third columns, and the magnification of a specific cell confirm that OPA1 is located in mitochondria. The white bar represents 10 μm. (**E**) OPA1, as determined by

immunoblotting, was detected in the fractions of light membrane (consisted mainly of endoplasmic reticulum) and mitochondria-associated membrane, which were separated using sucrose gradient ultracentrifugation. This phenomenon was particularly evident when expression of DRP1 or Mfn-2 was inhibited by siRNA.

Figure 3 Correlation between OPA1 expression and survival of LADC patients. (**A**) Expression of OPA1 was determined by immunoblotting. Expression of β-actin was used as a monitoring standard for the relative expression of OPA1. N: non-tumor lung tissue (NTLT), T: tumor fraction of surgical resections. (**B**) Representative examples of OPA1 expression in pathological specimens as detected by immunohistochemical staining (crimson precipitates). Expression of OPA1 was detected in (**B1**) the LADC tumor nest, but not in (**B2**) the NTLT. (**C**) Comparison of Kaplan-Meier product limit estimates of survival analysis in LADC patients. Patients were divided into 2 groups depending on the expression of OPA1. The difference in survival between the 2 groups was compared by the log rank test, and the *p* value was 0.0016.

Figure 4 Expression and post-translational modification of OPA1 in LADC cells. (**A**) Two bands of OPA1 protein were detected in LADC cells and pathological specimens by immunoblotting. However, RT-PCR showed that only one mRNA was detected in these samples, suggesting that the 110-kDa protein could be a phosphorylated OPA1. H23 cell lysate were treated with calf intestinal alkaline phosphatase (CIP) before immunoblotting; the 110-kDa protein band became less intense, while the 82-kDa protein band became more intense. (**B**) The effect of kinase inhibitor on OPA1phosphorylation. The H23 cells were treated with a panel of serine/threonine kinase inhibitors before immunoblotting. Only treatment with 5 μM calphostin C, a protein kinase C (PKC) inhibitor, reduced the intensity

of the 110-kDa and 82-kDa protein bands. The results suggested that the PKC-mediated phosphorylation was essential for maintaining OPA1 stability. (**C**) Different isozymes of PKC were ectopically expressed in H2009 cells before immunoblotting. Intensity of the 110-kDa protein increased in cells that ectopically expressed PKC. (**D**) Addition of 10 μM nicotine at 37°C for 4 h induced OPA1 phosphorylation. (**E**) Increase in OPA1 phosphorylation increased cisplatin resistance. ○, control H23 cells; ●, H23 cells treated with 10 μM of nicotine prior to cisplatin challenge.

Figure 5 OPA1 expression during cell cycle progression and serum starvation, and the association of its expression with cisplatin cytotoxicity. (**A**) OPA1 expression in different phases of cell cycle progression. HeLa cells were treated with double thymidine block (DTB) to synchronize cells at the late G1 phase. OPA1 levels increased about four hours (S phase) and decreased about 16 hours (G1 phase) after release from DTB. (**B**) H23 cells were cultured in medium containing 0.25% fetal calf serum (FCS) for 24-48 h, and OPA1 expression decreased at 48 h of serum starvation (left panel). OPA1 levels increased about 12 h (S phase) and decreased about 20 h (G1 phase) after addition of fresh FCS. (**C**) Knockdown of OPA1 expression by siRNAs ($OPA1^{kd}$) for 72 hours reduced the protein level of OPA1 in H23 cells as determined by immunoblotting analysis. (**D**) Silencing of OPA1 expression increased cisplatin sensitivity in H23 cells. ●, H23, wild-type; ○, H23, $OPA1^{kd}$. F-test, $p < 0.01$ (**E**) Serum-stimulated H23 cells were treated at different time point with cisplatin at 37°C for 4 h, wash twice with warm medium for 10 min, and then trypsinized. Viable cells were seeded quantitatively into 6-well plates with 5 ml of medium and incubated at 37°C and in 5% CO_2 over 7-10 days. Colonies were stained with 2% crystal violet in methanol. Percent survival was determined by comparison to PBS-treated controls. Results shown are from cells treated with 5 μM cisplatin. ○, H23 cells were cultured in 10% serum medium, wild-type; □,

H23, OPA1^{kd}; (**F**) Confocal fluorescence immunocytochemistry and (**G**) immunoblotting of sucrose gradient-separated organelle fractions showed that silencing of OPA1 increased cytoplasmic cytochrome c, but not cytoplasmic nor nuclear apoptosis-inducing factor (AIF) following treatment of cells with low dose (0.1 μM) of staurosporine (STS) for 4 hr, suggesting that OPA1 deficiency might increase caspase-dependent cell death. For retarding nuclear translocation of AIF, we also suppressed expression of human homolog of yeast Rad23A (hHR23A) by siRNA. (**H1**) Addition of low doses (0.1 or 0.25 μM) of STS for 4 hr provoked very diminutive effect on caspase 3 activation or degradation of poly (ADP-ribose) polymerase (PARP) in wild-type A549 cells. (**H2**) However, addition of sub-lethal doses (0.1 or 0.25 μM) of STS induced caspase 3 activation and PARP disintegration in OPA1^{kd} cells. It is worth noting that silencing of OPA1 increased non-specific degradation of PARP.

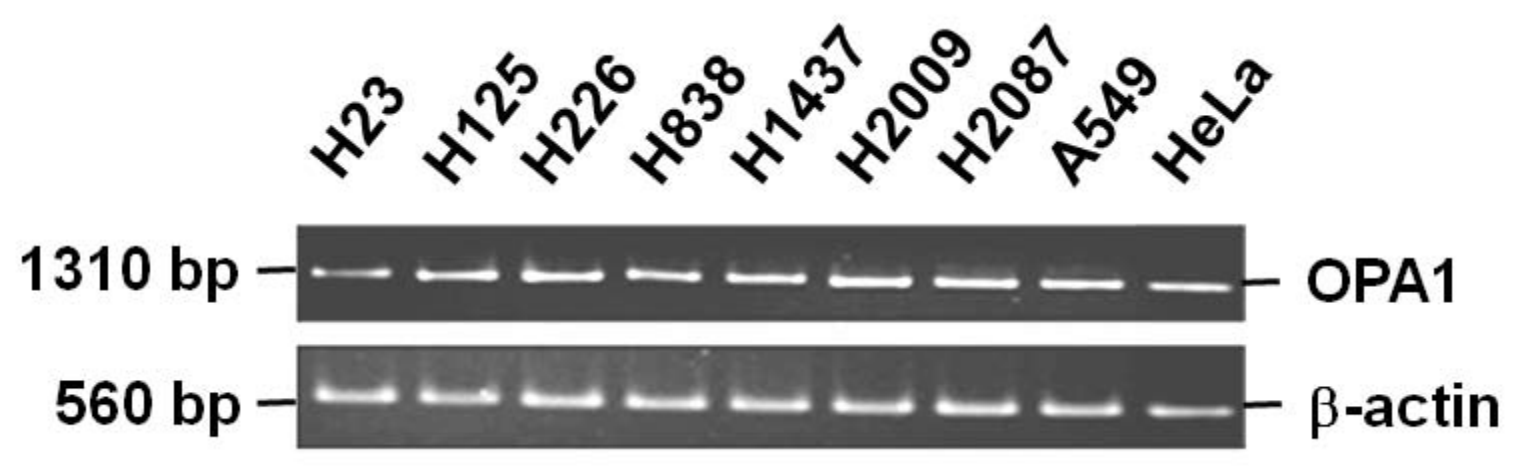
H23
H125
H226
H838
H1437
H2009
H2087
A549
HeLa
1310 bp
OPA1
560 bp
β-actin

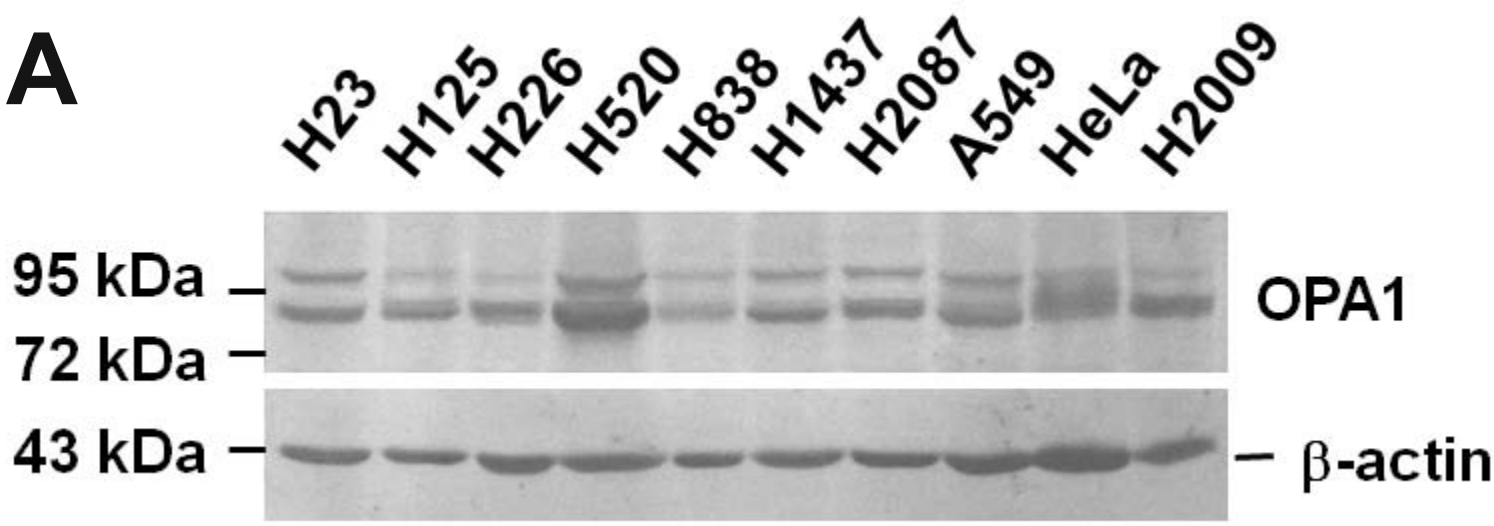
A
H23
H125
H226
H520
H838
H1437
H2087
A549
HeLa
H2009
95 kDa
72 kDa
43 kDa
OPA1
β-actin

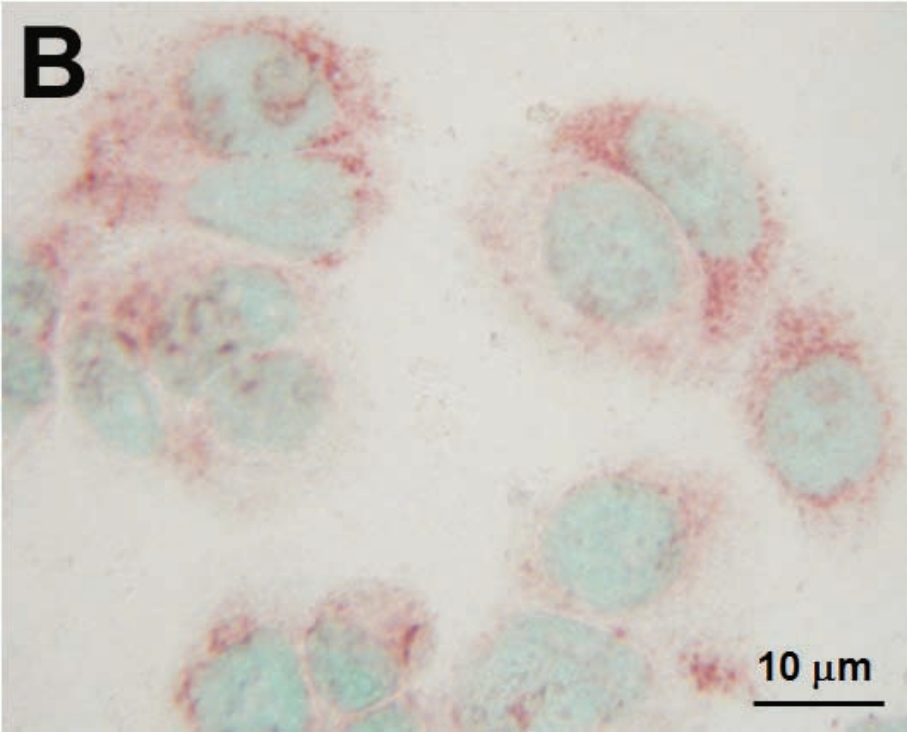
B
10 μm

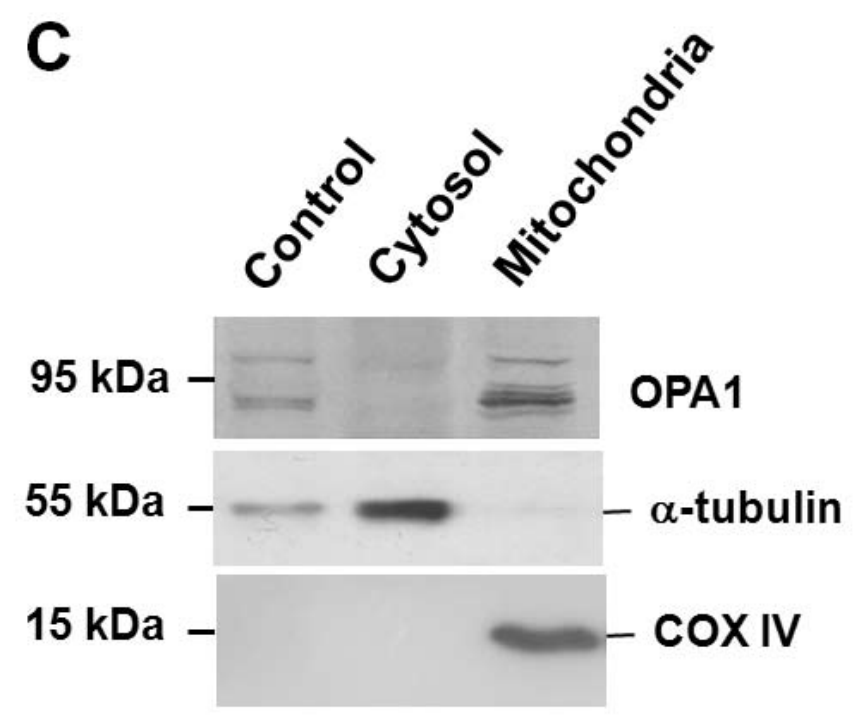
C
Control
Cytosol
Mitochondria
95 kDa
OPA1
55 kDa
α-tubulin
15 kDa
COX IV

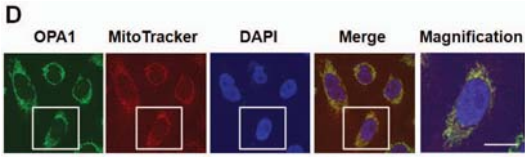
D
OPA1
MitoTracker
DAPI
Merge
Magnification

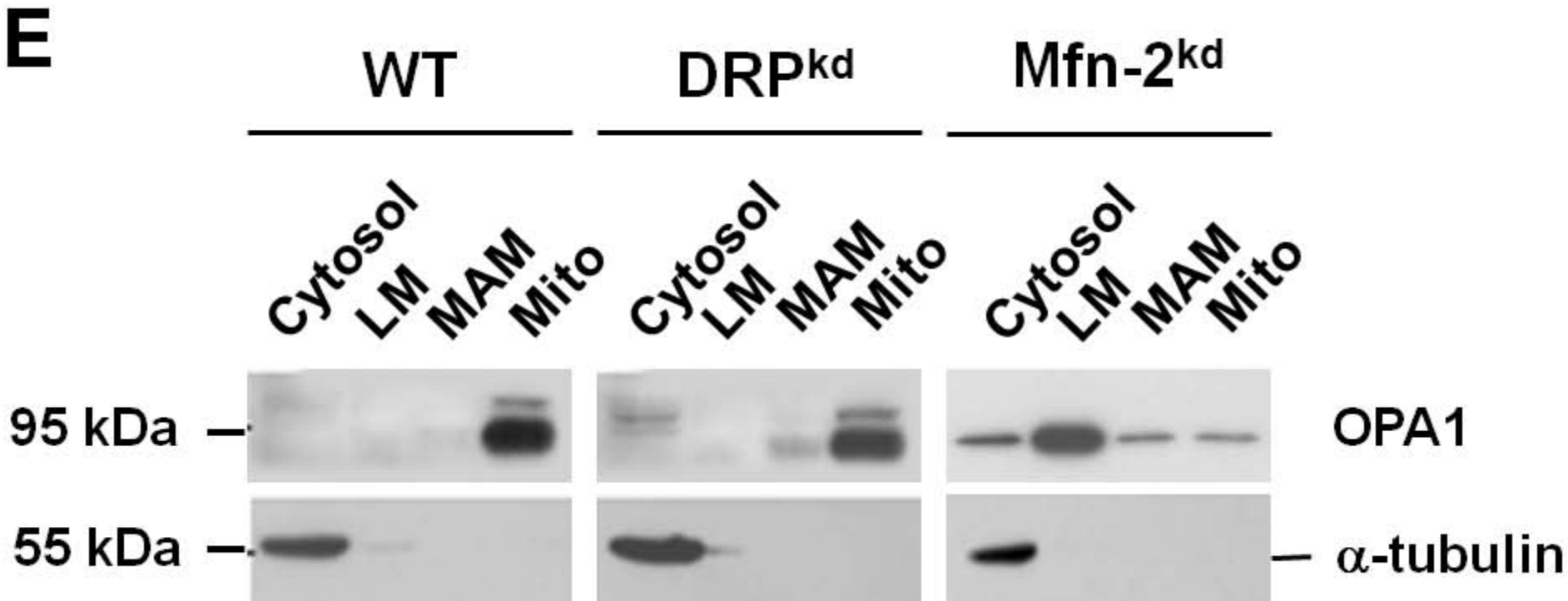
E
WT
DRPkd
Mfn-2kd
Cytosol
LM
MAM
Mito
Cytosol
LM
MAM
Mito
Cytosol
LM
MAM
Mito
95 kDa
OPA1
55 kDa
α-tubulin

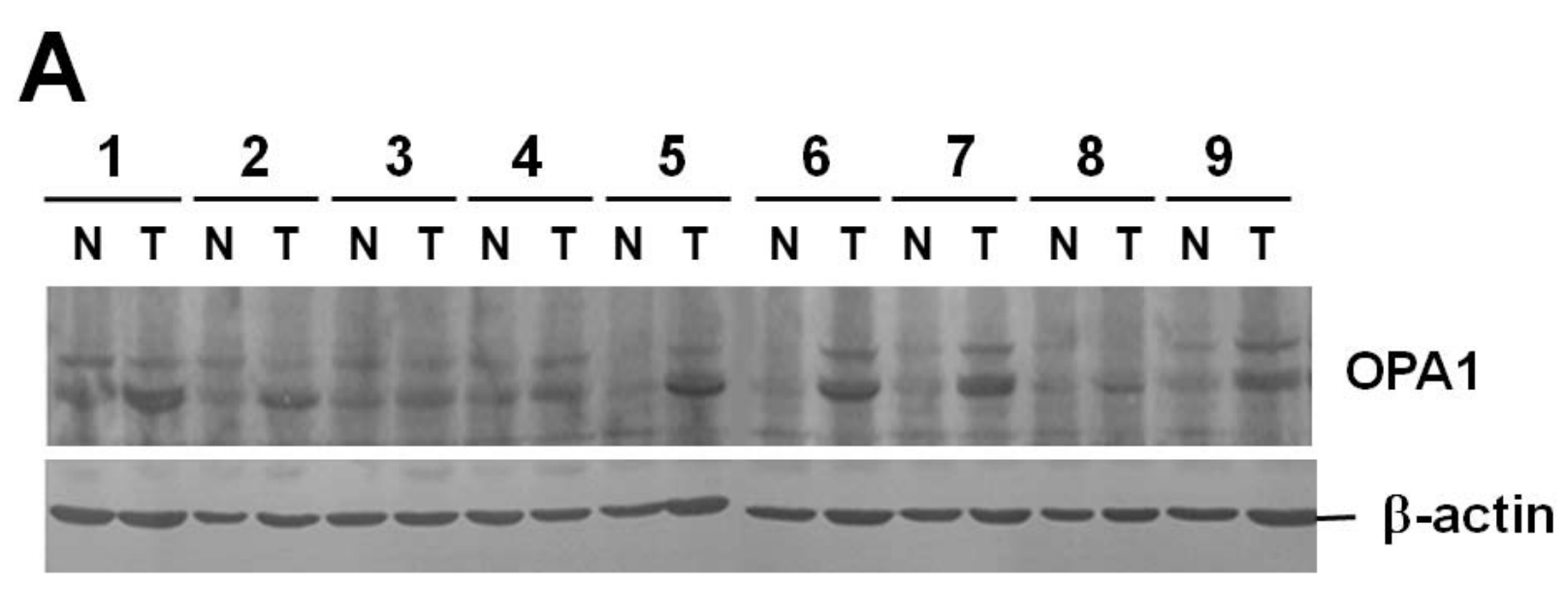
A
1
2
3
4
5
6
7
8
9
N T N T N T N T N T N T N T N T N T
OPA1
β-actin

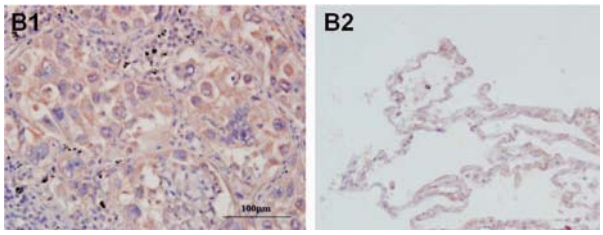
B1
100μm
B2

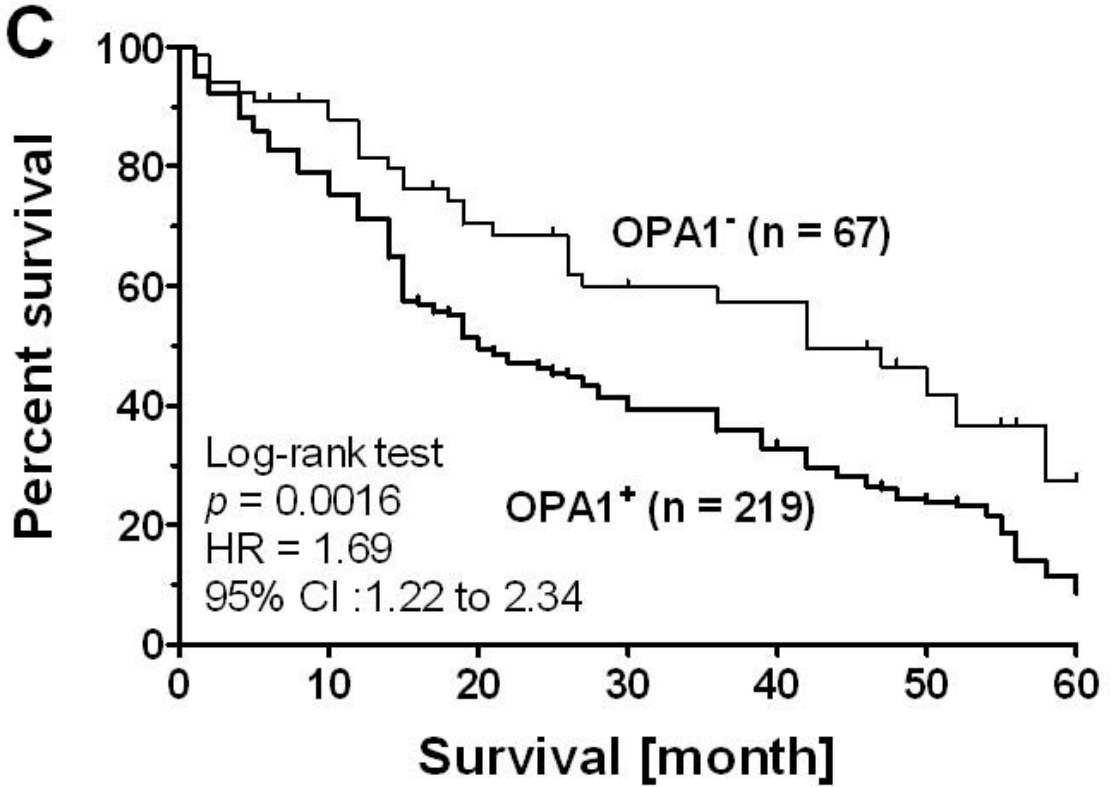
C
Percent survival
100
80
60
40
20
0
OPA1⁻ (n = 67)
OPA1⁺ (n = 219)
Log-rank test
p = 0.0016
HR = 1.69
95% CI :1.22 to 2.34
0
10
20
30
40
50
60
Survival [month]

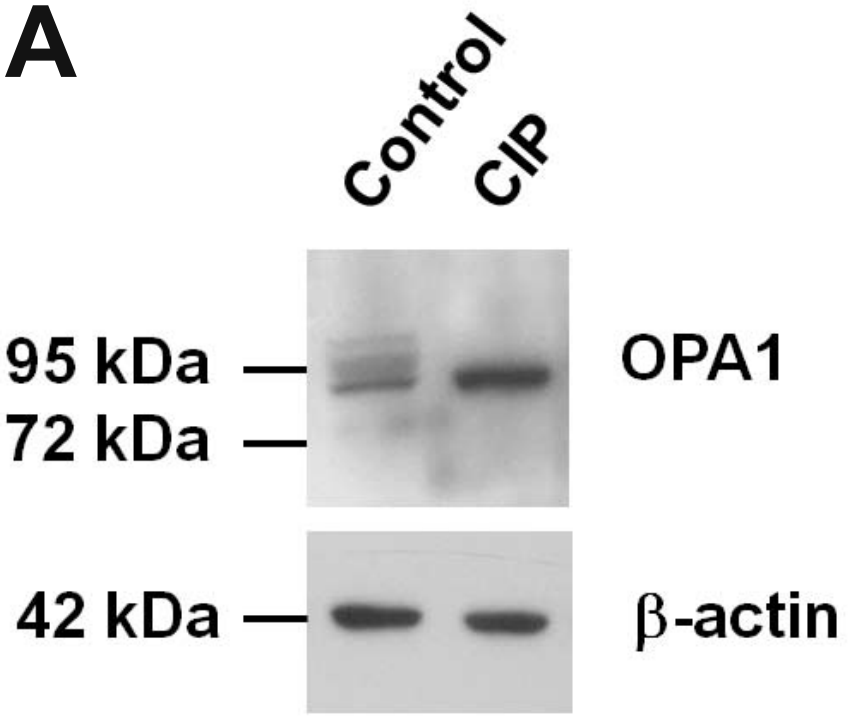
A
Control
CIP
95 kDa
72 kDa
OPA1
42 kDa
β-actin

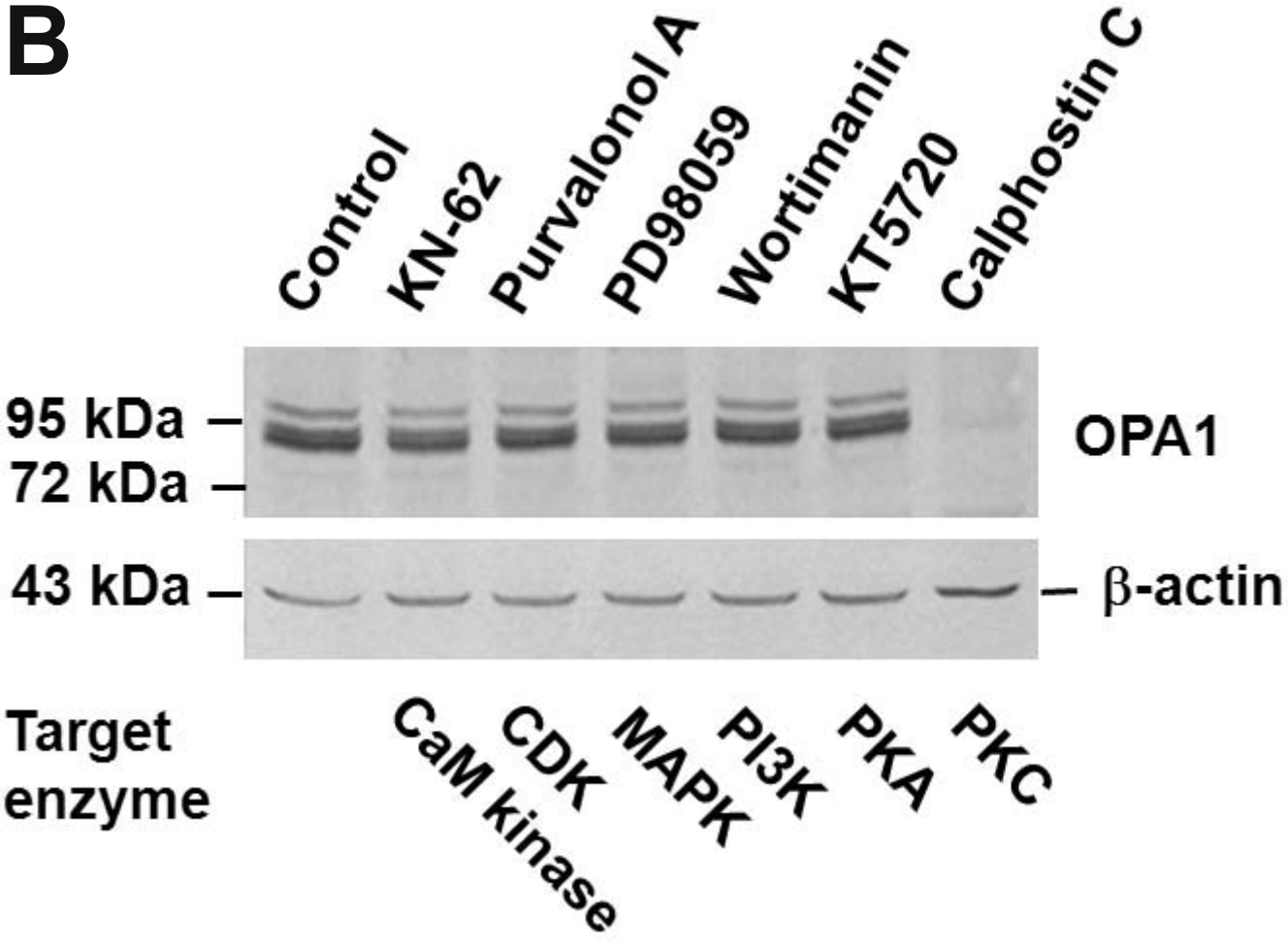
B
Control
KN-62
Purvalonol A
PD98059
Wortimanin
KT5720
Calphostin C
95 kDa
72 kDa
OPA1
43 kDa
β-actin
Target enzyme
CaM kinase
CDK
MAPK
PI3K
PKA
PKC

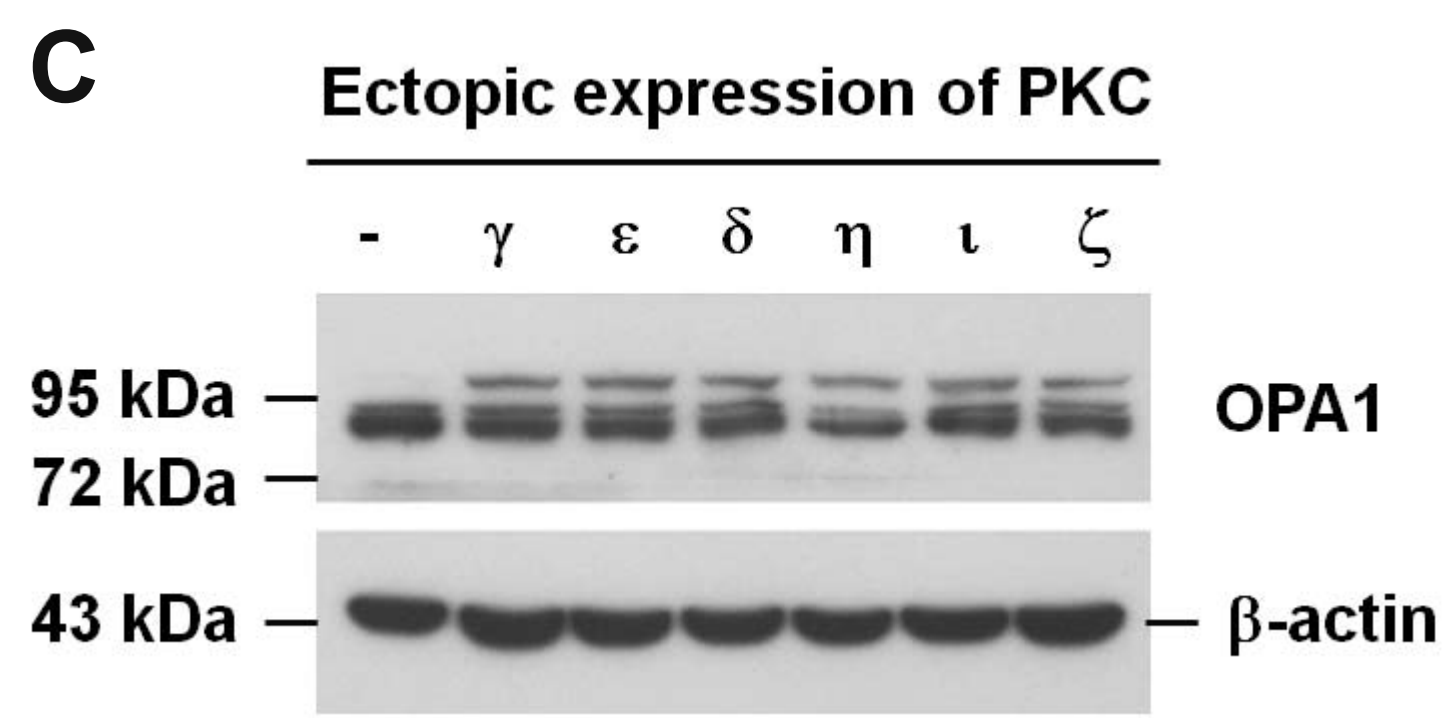
C
Ectopic expression of PKC
-
γ
ε
δ
η
ι
ζ
95 kDa
72 kDa
OPA1
43 kDa
β-actin

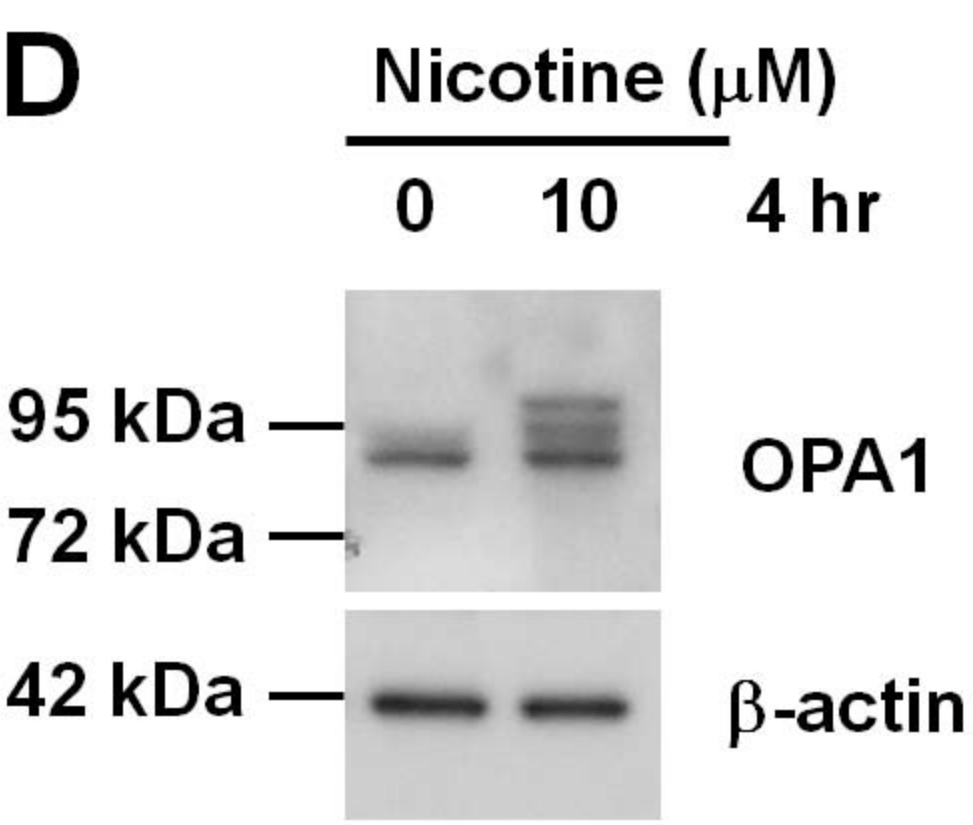
D
Nicotine (μM)
0
10
4 hr
95 kDa
72 kDa
OPA1
42 kDa
β-actin

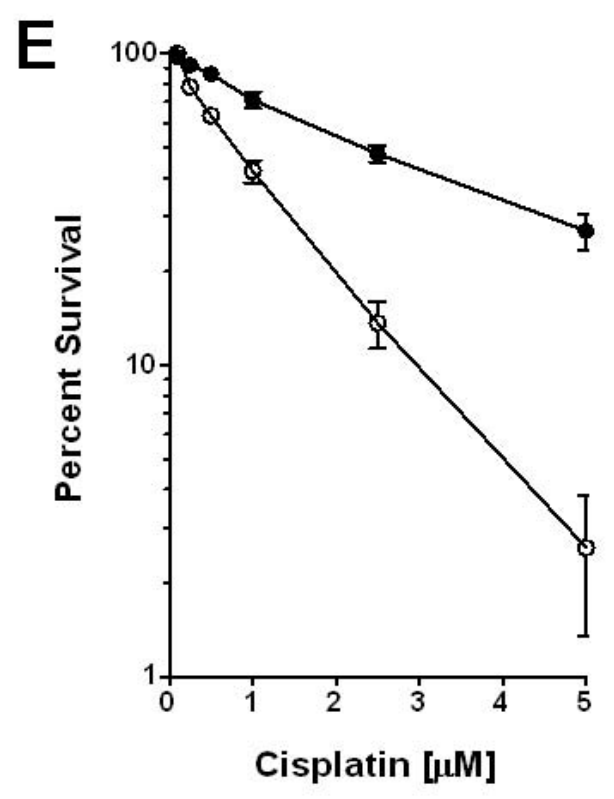
E
100
10
1
Percent Survival
0
1
2
3
4
5
Cisplatin [μM]

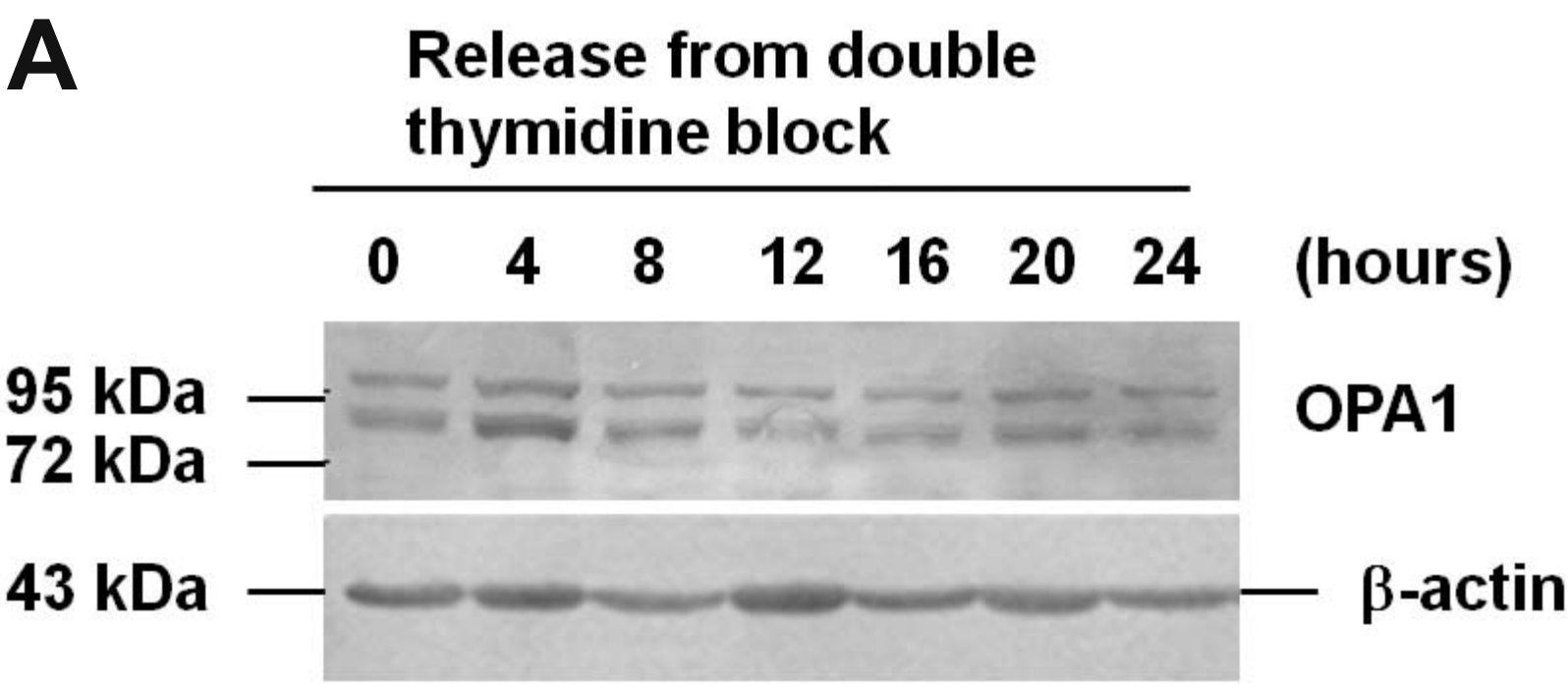
A
Release from double thymidine block
0
4
8
12
16
20
24
(hours)
95 kDa
72 kDa
OPA1
43 kDa
β-actin

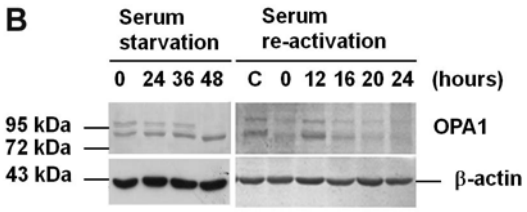
B
Serum starvation
Serum re-activation
0 24 36 48 C 0 12 16 20 24 (hours)
95 kDa
72 kDa
43 kDa
OPA1
β-actin

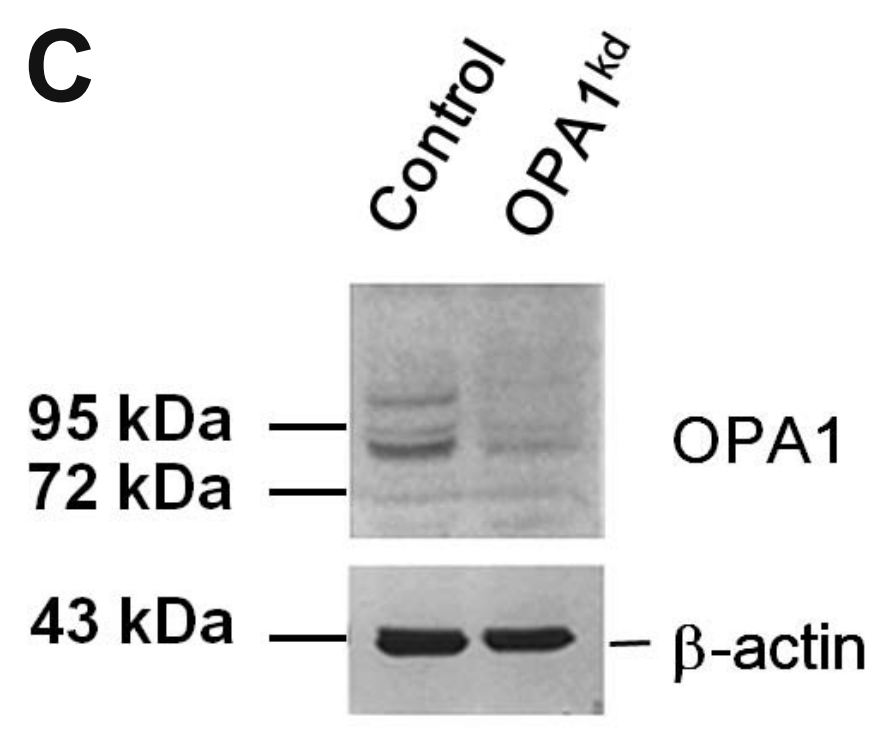
C
Control
OPA1kd
95 kDa
72 kDa
OPA1
43 kDa
β-actin

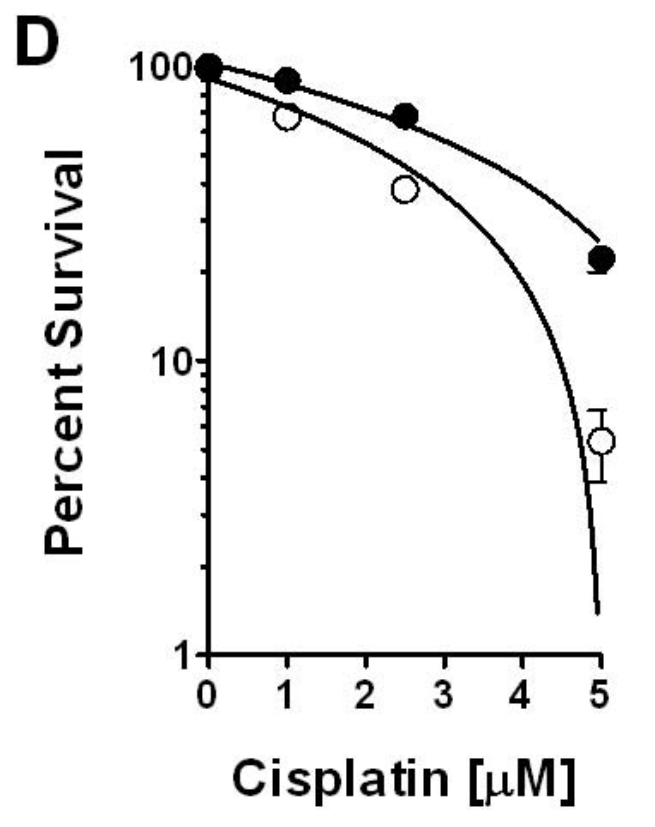
D
100
10
1
Percent Survival
0
1
2
3
4
5
Cisplatin [μM]

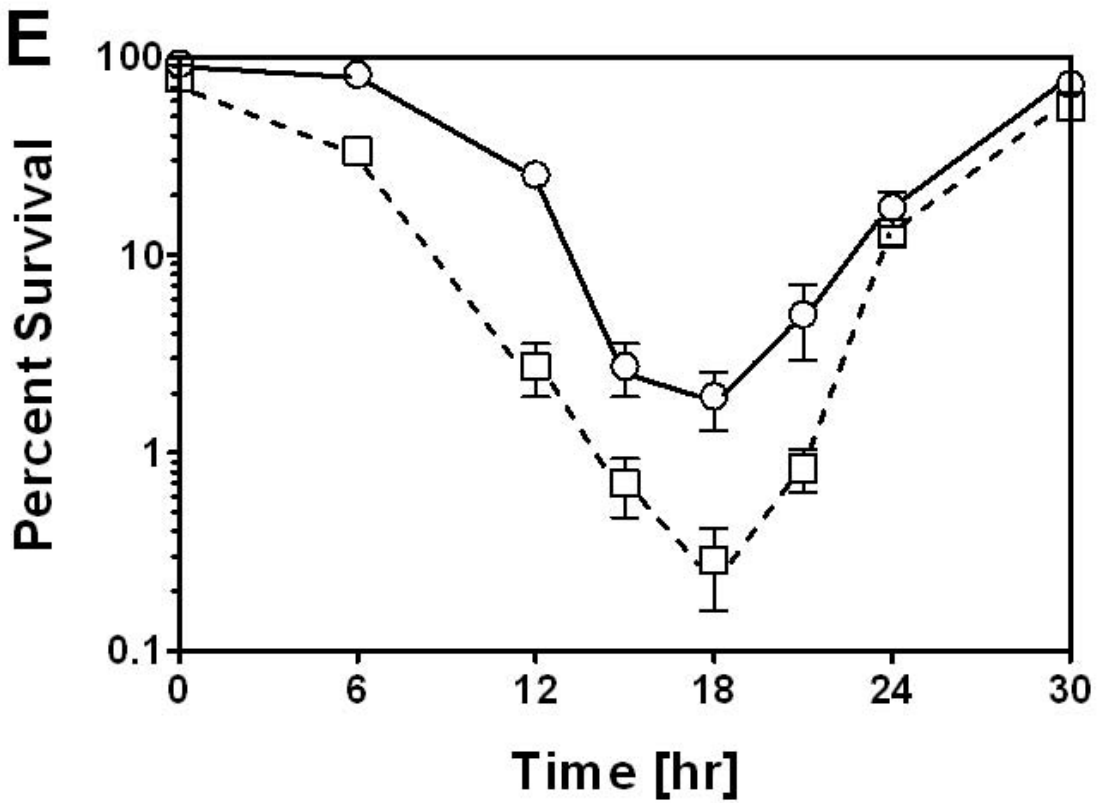
E
Percent Survival
100
10
1
0.1
0
6
12
18
24
30
Time [hr]

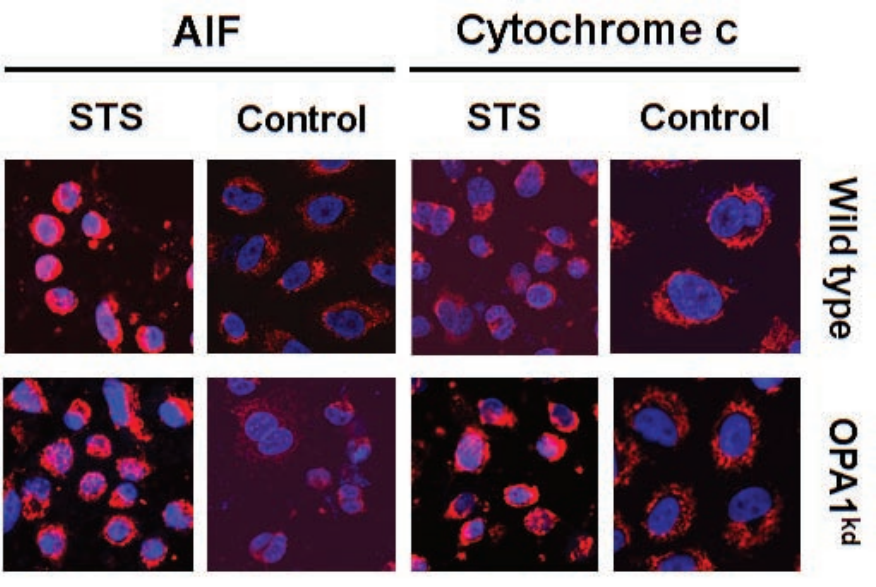
AIF
Cytochrome c
STS
Control
STS
Control
Wild type
OPA1kd

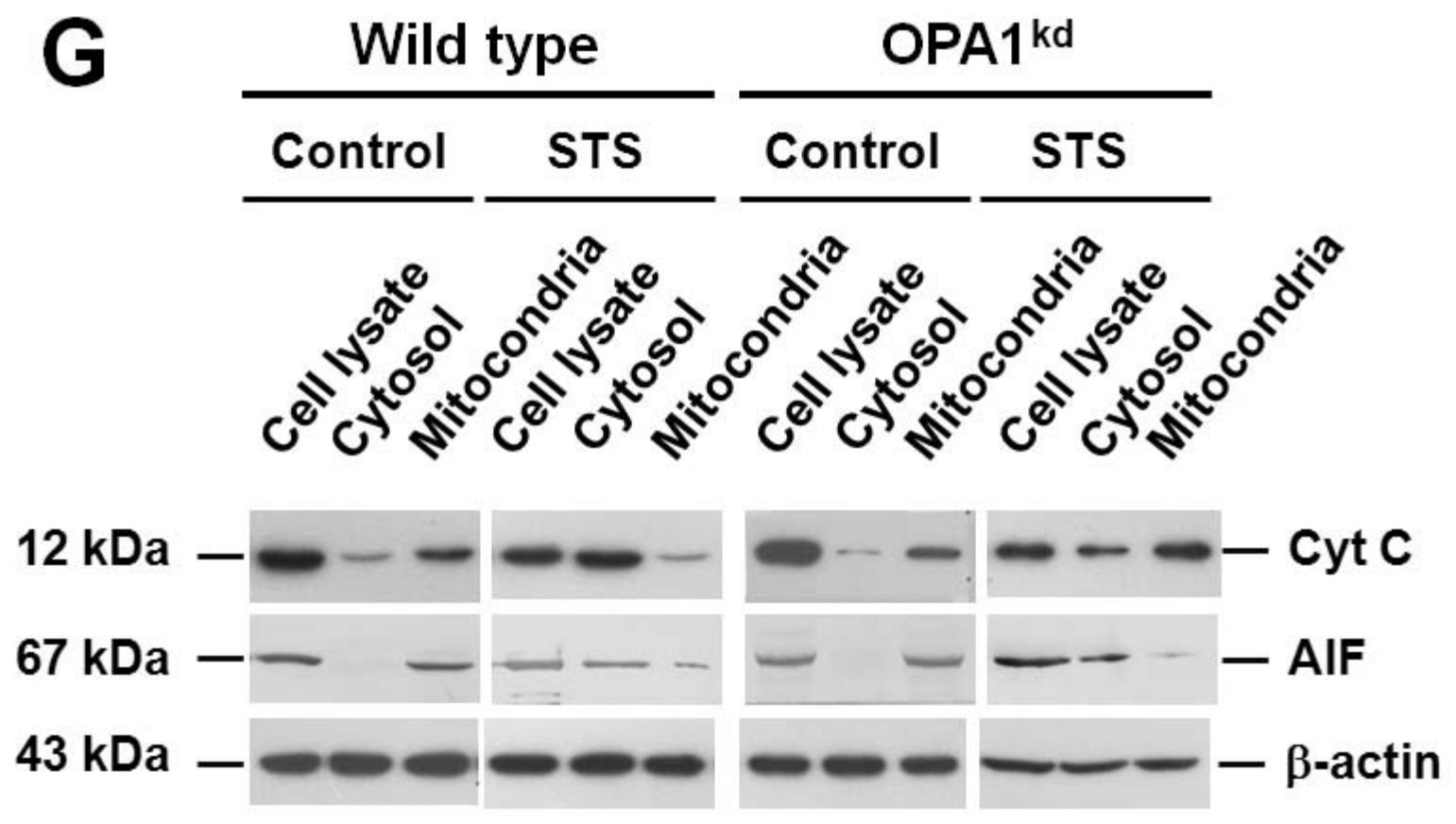
G
Wild type
OPA1kd
Control
STS
Control
STS
Cell lysate
Cytosol
Mitocondria
Cell lysate
Cytosol
Mitocondria
Cell lysate
Cytosol
Mitocondria
Cell lysate
Cytosol
Mitocondria
12 kDa
67 kDa
43 kDa
Cyt C
AIF
β-actin

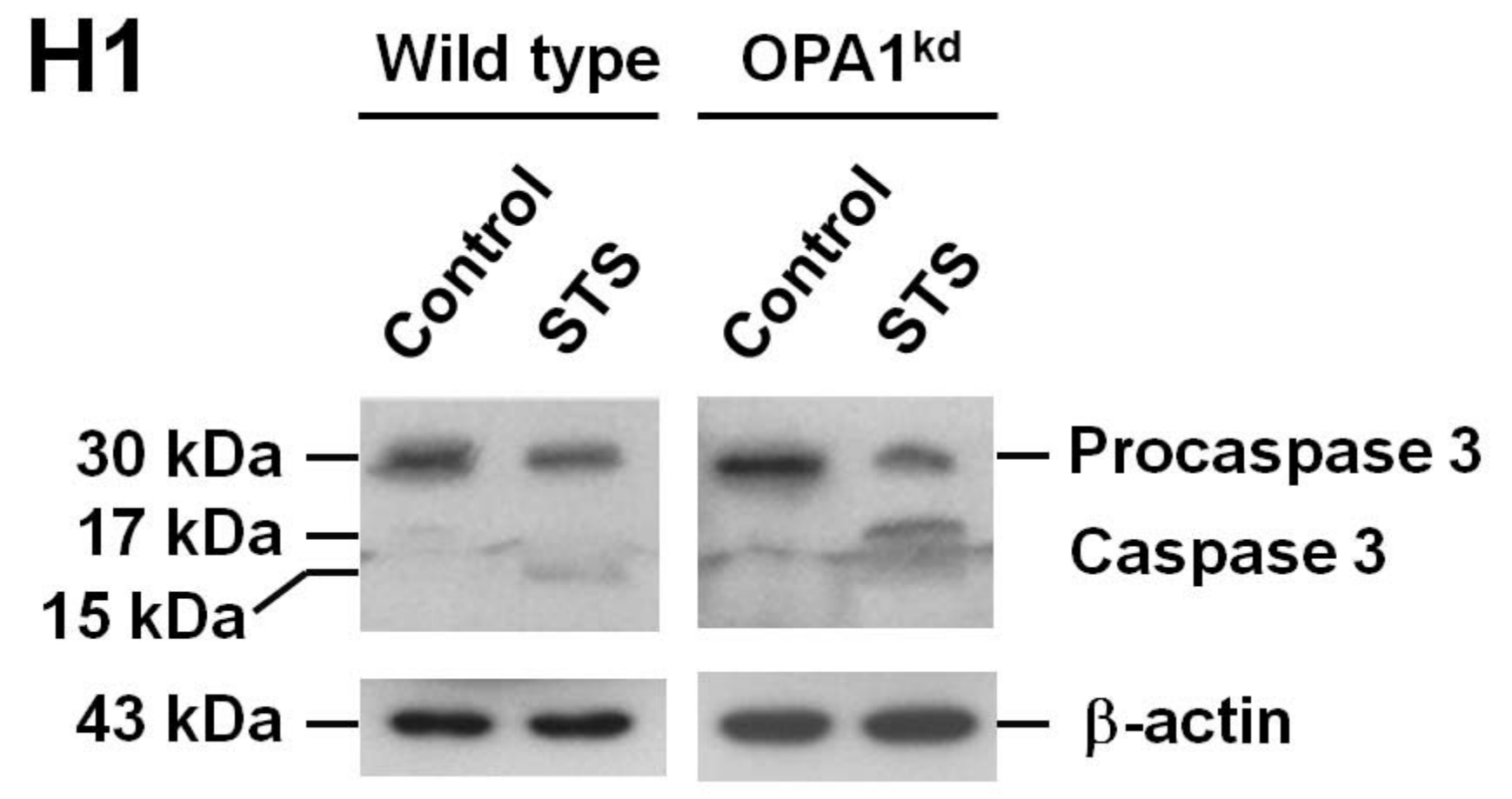
H1
Wild type
OPA1kd
Control
STS
Control
STS
30 kDa
17 kDa
15 kDa
Procaspase 3
Caspase 3
43 kDa
β-actin

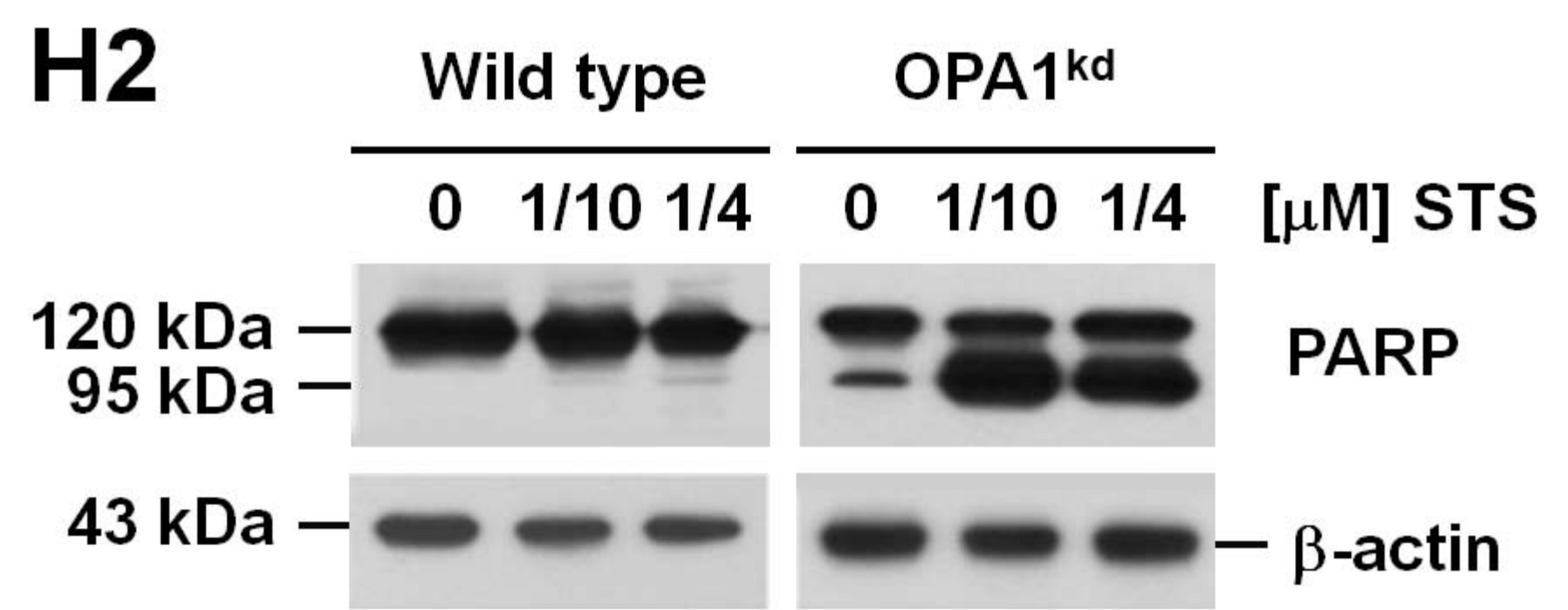
H2
Wild type
OPA1kd
0
1/10
1/4
0
1/10
1/4
[μM] STS
120 kDa
95 kDa
PARP
43 kDa
β-actin

Table 1. Correlation of OPA1 expression with clinicopathological parameters in LADC patients

Parameter	Expression of OPA1		*p* value/correlation[§]
	High (n = 219)	Low (n = 67)	
Gender			
Male (n = 224)	178	46	0.041[†]/0.13
Female (n = 62)	41	21	
Cigarette Smoking			
Smoker (n = 154)	139	15	< 0.001[†]/0.35
Non-smoker (n = 132)	80	52	
Stage			
I (n = 89)	81	8	<0.001[‡]/0.44
II (n = 122)	101	21	
III (n = 75)	37	38	
Cell differentiation			
Well (n = 39)	27	12	0.504[‡]/-0.052
Moderate (n = 169)	131	38	
Poor (n = 78)	61	17	
Lymphovascular invasion			
Positive (n = 216)	178	38	< 0.001[†]/0.242
Negative (n = 70)	41	29	
Expression of AKR1C1/2			
AKR1C1/2^{+} (n = 237)	208	29	< 0.001[†]/0.581
AKR1C1/2^{-} (n = 49)	11	38	

mitochondria-associated proteins			
$DRP1^{nuc+}$ (n = 226)*	191	35	< 0.001†/0.364
$DRP1^{nuc-}$ (n = 60)*	28	32	
$ATAD3A^{+}$ (n = 242)	212	30	< 0.001†/0.611
$ATAD3A^{-}$ (n = 44)	7	37	
Mfn-1^{+} (n = 203)	191	12	< 0.001†/0.647
Mfn-1^{-} (n = 83)	28	55	
Mfn-2^{+} (n = 177)	158	19	< 0.001†/0.382
Mfn-2^{-} (n = 109)	61	48	

†Two-sided *p* value determined by χ^2 test

‡Two-sided *p* value determined by Fisher's exact test

*Nuclear expression of DRP1 labeled as $DRP1^{nuc+}$; Cells which did not express DRP1 or the DRP1 was in the cytoplasm was labeled as $DRP1^{nuc-}$.

§The value was determined by the Spearman Correlation, which was based on normal approximation, and not assuming the null hypothesis.